THE UNIVERSITY OF MANITOBA

EFFECT OF PRIOR FATIGUE ON THE CRACK PROPAGATION RATES IN THREE HIGH STRENGTH SHEET MATERIALS

by

M. N. CLARK

A THESIS

SUBMITTED TO THE FACULTY OF GRADUATE STUDIES

IN PARTIAL FULFILMENT OF THE REQUIREMENTS FOR THE DEGREE

MASTER OF SCIENCE IN ENGINEERING

DEPARTMENT OF MECHANICAL ENGINEERING

WINNIPEG, MANITOBA

February, 1972

ABSTRACT

Plane stress crack propagation studies using centrally notched specimens were conducted on three typical airframe materials (2024-T3 & 7075-T6 Alclad alloys and Ti-6Al-4V) to evaluate the effect of fatigue damage prior to the formation of a crack on the subsequent crack propagation rate.

The specimens were subjected to fatigue damage by strain cycling at a constant amplitude to a number of cycles less than the endurance. The crack growth in these damaged specimens was compared to that in undamaged control specimens. The crack growth rate was evaluated by performing an exponential regression analysis on the observed data.

The comparison of the crack length and the crack growth rate of the damaged with the undamaged revealed a definite trend towards faster crack growth in the damaged 2024-T3 alloy; this effect was apparent only after transition from the tensile to the shear mode of failure. No such trend was observed in either the 7075 or titanium tests. It was further observed that only the 2024 specimens exhibited necking ahead of the crack tip and it was sugested that ductility played a major role in the effect of fatigue damage on the subsequent crack propagation rate.

ACKNOWLEDGEMENTS

The author wishes to express his sincere appreciation to his advisor Dr. J. Shewchuk for his guidance and encouragement throughout the project. Acknowledgement is also due the Defence Research Board for their support under DRB Grant 9535-48 to Dr. Shewchuk and for granting the author an Educational Leave of Absence to pursue these studies. Finally, the author would like to extend his thanks to his fellow students and to the technicians at the University of Manitoba for their help throughout the course of these studies.

CONTENTS

LIST OF FIGURES

NOMENCLATURE

a	crack half length	(in. or mm.)
A	cross sectional area	(in^2)
c_w	finite width correction factor	-------
daN	deca newtons	(metric force)
exp( )	base e - $e^{( )}$	-------
$\mathcal{G}$	crack driving force	-------
K	stress intensity factor	(ksi $\sqrt{in}$)
K_{Ic}	fracture toughness	(ksi $\sqrt{in}$)
ΔK	alternating stress intensity factor	(ksi $\sqrt{in}$)
ℓ	crack length	(in. or mm.)
m	ratio crack length/plate width	-------
n	kilocycles	-------
N	cycles	-------
α,β,γ	regression coefficients	-------
σ	gross section stress	(psi)
$\Delta\sigma,\sigma_a$	alternating stress	(psi)
σ_m	mean stress	(psi)

CONVERSION FACTORS

With the increasing adoption of the International System of Units (SIU) for measurements, much of the data published is being presented in these units. A short summary of the conversion factors between this system and the British in-lb system is therefore included below; only those terms frequently used within this report are given.

in	× 25.400 =	mm	mm	× $.394 \cdot 10^{-1}$ =	in
in^2	× 645.160 =	mm^2	mm^2	× $1.550 \cdot 10^{-3}$ =	in^2
ksi	× 6.895 =	N/mm^2	N/mm^2	× .145 =	ksi
$ksi\sqrt{in}$	× 3.475 =	$daN/mm^{3/2}$	$daN/mm^{3/2}$	× .288 =	$ksi\sqrt{in}$
lbf	× 4.448 =	N	N	× .225 =	lbf
psi	× 6894.760 =	N/m^2	N/m^2	× $1.450 \cdot 10^{-4}$ =	psi

1.0 INTRODUCTION

1.1 BACKGROUND

While the phenomenon of material degradation due to cyclic loading (fatigue) has been recognized since late in the last century, most studies have been confined to the establishment of S-N curves for use in engineering design. While such data do afford a basis for design, the statistical variation is rather broad and a reliable design is, by necessity, very conservative. Furthermore, since the data is obtained in the form of cycles to failure (sudden and complete fracture of the specimen), no indication of impending failure is available. In instances where sudden failure could be dangerous but where the structural member must sustain high loads (from weight considerations etc.), it is necessary to adopt the fail safe approach wherein the design is redundant and failure of one member would not be catastrophic.

In addition, most tests are conducted using laboratory specimens and it is difficult to relate these data to real structures. The data is therefore used with caution and the design is further evaluated by full scale testing - a very time consuming and costly approach.

Attempts to study the mechanism of fatigue with the aim of being able to predict failures more accurately have met with very limited success. These studies, however, have dealt with the microscopic nature of fatigue and the results do not lend themselves directly to engineering applications.

The problem of brittle fracture wherein a ductile material fails in a brittle manner at stresses far below the yield strength in the

absence of strain cycling proved to be the catalyst in directing the research towards a better understanding of the macroscopic nature of fatigue. Although the phenomenon of brittle fracture is not necessarily associated with fatigue, studies into its nature led to the development of the theories of FRACTURE MECHANICS which in turn can be used to explain and predict fatigue failures. The development and use of these theories as applied to fatigue are detailed in Chapter 2.

1.2 FRACTURE MECHANICS APPLIED TO FATIGUE

Extensive studies have shown that the mechanism of fatigue is comprised of several stages:

(i) Plastic slip along the slip planes of grains.

(ii) Formation of microcracks along the slip planes of grains.

(iii) Joining of microcracks.

(iv) Growth of microcracks until failure.

Figure 1 illustrates these stages on a non-dimensionalized S-N curve. Final failure occurs when the crack has grown to such an extent that the remaining area will not sustain the applied load; sudden and brittle fracture then occurs. In this sense, a fatigue failure is a static failure preceded by crack initiation and propagation.

As will be shown in Chapter 2, the crack growth phase and the time to subsequent fracture are very predictable and can be readily divorced from size and geometry effects. The variability in the S-N curve is largely a result of the crack initiation phase. A detailed knowledge, therefore, of the crack propagation and failure stages is very useful in engineering design. With careful application, a structure can be designed much more confidently with a saving in weight by supplementing

the S-N data with fracture mechanics properties. For such a procedure however, considerable care must be taken not only in the design but also in subsequent in-service inspections. For example, should one design for a life of N_1 cycles using the S-N curve with appropriate confidence limits (as shown in Figure 2), an allowable stress of σ_1 might be dictated. If, however, one could accept rigorous in-service inspections at periodic intervals, a stress of σ_1' might be specified accompanied with inspections beginning at some time less than N_1'. Since the crack propagation and failure stages are considerably more predictable than the initiation stage, the detection of a crack would mean that the cause of the variability had passed and that the principles of fracture mechanics could be used to evaluate the remaining life. The inspection intervals and the minimum flaw size which must be detected would be dictated by fracture mechanics principles.

1.3 SCOPE OF PRESENT STUDY

In order to confidently predict the life during the crack propagation phase, one must know the effects of any variables which are likely to be encountered in service. One such variable is the material history. Cracks will usually start at the surface in the region of a stress concentration, and it is quite conceivable that a component could be subjected to a considerable proportion of its service life before the concentration were induced (as a scratch, nick etc.). Conversely, a sharp stress raiser will initiate a crack sooner than a blunt one and the material some distance from the blunt raiser will have sustained more fatigue damage by the time a crack has formed. The question then arises-"Will this fatigue damage affect the subsequent crack propagation?"

An experimental program was conducted to evaluate this effect and forms the basis for this thesis.

Prior to discussung the specific study conducted, a brief resumé of the underlying principles of fracture mechanics will be presented together with a summary of previous work done in the area of crack growth.

2.0 FUNDAMENTALS OF FRACTURE MECHANICS

A detailed treatment of the concepts of fracture mechanics is beyond the scope of this thesis; the reader is referred to Chapters 4 & 5 of Barrois(1)* for a thorough presentation of these principles. A brief summary is presented here since the experimental program is based upon these concepts.

2.1 FAILURE THEORIES

As stated earlier, metallic fatigue consists of crack initiation, crack growth and fracture. Fracture occurs in a brittle manner at a net section stress much lower than the yield strength of the material. Experience gained in service has shown that very small cracks (from fatigue, corrosion, quench shrinkage etc.) can reduce the static strength of components by 20 to 30%. This problem is more severe in the ultra high strength alloys,which tend to be brittle,than in the more ductile low strength alloys. Brittleness, however, is also a function of the crack length and the high strength alloys usually have properties aside from their strength which are desirable.

To characterize the brittleness of a material in its service condition when a crack has formed, some quantity which is invariant for a given combination of material, geometry and crack size is required. Griffith (2) proposed, for highly brittle materials, that this invariant quantity is given by the crack driving force $\mathcal{G}$ (defined as the surface density of the elastic energy (U) released due to the increase in the

---

* Bracketed numbers in the text refer to references listed in Chapter 6

surface area of the cracked section).

$$\mathcal{G} = \frac{dU}{dA} \quad \text{---------- (1)}$$

Fracture occurs when the energy released exceeds the surface tension (T).

$$\text{i.e. } \mathcal{G} \geq 2T \quad \text{---------- (2)}$$

$$\text{where } T = \frac{1}{2}\frac{dW}{dA} \quad \text{---------- (3)}$$

W = total decohesion work

This condition of failure is termed critical and is denoted by $\mathcal{G}_c$. This concept of failure, however, is not readily applied to less brittle materials because of the inadequacy of the term "surface tension" and the difficulty in readily measuring its magnitude.

For thin sheets, Irwin (3) introduced the concept of stress intensity factor (K) given by:

$$K^2 = E\mathcal{G} \quad \text{---------- (4)}$$

where K is a function of the external load, the crack length and the geometry. Failure occurs at a critical stress intensity factor K_c and K_c approaches the lower limit K_{Ic} as the specimen thickness increases. Figure 3 illustrates this thickness effect for three typical materials. The limit K_{Ic} is termed the FRACTURE TOUGHNESS and has been shown to be an invariant for a given material.

If the crack and load are such that $K<K_c$, the material will withstand the load until such time as the crack propagates (through cyclic loading or an aggressive environment) and results in K approaching critical. When $K = K_c$, fracture occurs suddenly.

For examples on the application of fracture mechanics to design, the reader is referred to Tiffany & Masters (23).

2.2 STRESS ANALYSIS OF CRACKS

Considerable effort has been expended in the development of analytical relationships to evaluate the stress intensity factor for various shapes and loading configurations. The derivations of these expressions is beyond the scope of this thesis; a catalogue of solutions may be found in Barrois (1) and Paris & Sih (24).

For a transverse through crack in a thin sheet of infinite width loaded in uniaxial tension the stress intensity factor is given by:

$$K = \sigma\sqrt{\pi a} \quad \text{---------- (5)}$$

where: σ = gross section stress in the absence of the crack

a = crack half length

The effect of the finite width of any specimen may be accounted for by the use of a correction factor c_w.

i.e. $$K = \sigma\sqrt{\pi a}\cdot c_w \quad \text{---------- (5a)}$$

For a central transverse crack in a sheet of finite width w, Isida (4) suggests the correction factor:

$$c_w = \{(1+.5948m^2+.4812m^4+.3963m^6+.3367m^8+.2972m^{10}+.2713m^{12} +.2535m^{14})\}^{.5} \quad \text{---------- (6)}$$

Baharandi (5) suggests the finite width correction factor:

$$c_w = (1-m^2)^{-.5} \quad \text{---------- (6a)}$$

where $m = (2a)/w$ in both expressions

Elongation measurements (by Baharandi) made at at least six locations ahead of the crack tip to evaluate the stress intensity factor are compared with those calculated using both Isida's and Baharandi's expressions in Figure 5. From this comparison it can be seen that Isida's method yields a slightly higher value for K and is a

better approximation than Baharandi's.

Expressions similar to those in equations 5 & 6 have been developed for various other combinations of crack shape, specimen geometry and loading manner.

2.3 SUBCRITICAL FLAW GROWTH

If the stress intensity factor is less than critical, the component will withstand the applied load until the crack grows to such a length that $K = K_c$. This period of crack growth is termed SUBCRITICAL FLAW GROWTH.

2.3.1 Mechanisms

The mechanism of crack propagation is relatively complex and is not yet completely understood. However, at the crack front the high stress concentration results in a zone of plastic strain (Figure 6) which gives rise to a residual compressive stress upon unloading. Under constant amplitude stress the crack front progresses at each cycle during the load-rise sequence and upon unloading the crack closes as shown in Figure 7. During this compressive phase it is assumed that shear causes damage to the still uncracked material; the damaged area is larger the higher the alternating stress. Upon loading, the crack extends into the damaged area and comes to a stop when reaching a less damaged area of the material. This results in the striations observed on fatigued components.

Referring to Figure 8, the crack begins at a point of incipient weakness and remains plane as it propogates in a direction normal to the maximum tensile stress. Such a crack is termed a tensile mode of failure. For a constant alternating stress (σ_a) far above and below the crack plane, the mean stress (σ_m) in the still uncracked section

and the stress intensity factor near the crack front increase with crack length hence the crack progresses at an increasingly faster rate and the distance between the striations increases. Intermittant crack growth by big leaps (corresponding to a partial static failure) is sometimes observed.

As the crack progresses, shear lips form at 45°; the width of the lips increases slowly with the mean stress finally extending through the thickness unless failure occurs beforehand. A crack with fully developed shear lips is said to be a shear mode of failure.

Wilhem (6) has investigated this transition from the tensile to the shear mode and has found that it corresponds to a knee in the curve obtained by plotting the crack propogation rate versus the alternating stress intensity factor on a semi-logarithmic scale. This knee is readily discernible in Figure 11 at a crack propogation rate of slightly less than 10^{-5} in/cycle.

2.3.2 Correlation

Of prime interest to the engineer is the crack growth per cycle or CRACK PROPOGATION RATE (da/dN) as a function of the stress intensity factor. Donaldson and Anderson (7) have shown that the best correlation is obtained using the alternating stress intensity factor (ΔK); their results are presented as Figures 9 and 10.

In an attempt to formulate a mathematical expression for the crack propogation rate, Broek et al (31) observed that the best correlation was obtained using a power of the alternating stress intensity factor:

$$da/dN = C\Delta K^n \qquad \text{---------- (7)}$$

This expression has also been used by other investigators with a value

of n between 2 and 3 being the most commonly reported. It should be noted that this expression applies only after the transition to the shear mode of failure (i.e. at the higher crack propogation rates).

2.3.3 Effect of Load

Paris (8) investigated the effect of type of load. His results are presented as Figure 11 wherein he demonstrates that a uniform loading some distance from the crack and a wedge type of load on the crack produce the same crack propagation rate for the same alternating stress intensity factor. For clarity, Paris omits the finite width correction factor in calculating ΔK.

i.e. For the case of the central transverse crack in a uniform tensile stress field:

$$\Delta K = \Delta\sigma\sqrt{a} \quad \text{---------- (8)}$$

and for the wedge loaded crack:

$$\Delta K = \frac{\Delta F}{\pi\sqrt{a}} \quad \text{---------- (8a)}$$

2.3.4 Effect of Mean Stress

Although the mean stress does affect the crack propagation rate to some degree, it is generally considered that it is of secondary importance compared to the alternating stress. Frost and Dugdale (9) tested a mild steel at four values of the mean stress and did not find any significant effect although they did find some effect for an aluminum alloy. Their results indicated a crack propagation law of the form:

$$da/dN = C \cdot \sigma_m^{\gamma} \cdot \sigma_a^{\beta} \cdot a^{\alpha} \quad \text{---------- (9)}$$

where C, γ, β & α are material dependent constants

Extensive studies by Broek and Schijve (10) using both 2024-T3 and 7075-T6 aluminum alloys supported this relationship and suggested

that the crack propogation rate is proportional to a power of the mean stress in the order of 1.5 {i.e. $\gamma \simeq 1.5$ in eqn. (9)}. Figure 12 is typical of their results. They also observed that the more ductile the aluminum alloy, the lower the crack propogation rate.

2.3.5 Effect of Stress Range

The effect of stress range ($\Delta\sigma$) has been evaluated by Lehr and Liu (11), McEvily and Illg (43), Wei et al (44) and Hudson (45) among others. All have concluded that, at a constant mean stress, the crack propagation rate is a function of the alternating stress intensity factor regardless of the alternating stress range. Typical results by McEvily and Illg for a 2024-T4 aluminum alloy are presented as Figure 13.

2.3.6 Effect of Frequency

Frequency effects were evaluated by Hartman et al (12) for a clad 2024-T3 sheet in both dry and saturated air. In both instances they observed a slight trend towards a higher crack propagation rate at lower frequencies. Similar results were reported by Schijve et al (13) and by Illg and McEvily (14). In all cases the shift in the crack propagation rate due to frequency was approximately 30 to 40% greater at 13 cpm than at 1200 cpm. Typical results by Hartman are included in Figure 14.

2.3.7 Random Loading and Overloading

Since, in real life, structures very seldomly experience the constant amplitudes used in laboratory testing, the effects of random loading and of overloading must be known if the designer is to make accurate use of the laboratory results.

Schijve (15) investigated the latter and observed that if overloads are applied in the course of crack growth, each group of these overloads

(1 to 3 cycles) will at first cause a delay of crack growth after which crack extension tends to continue at the rate it would assume in the absence of peak loads. Figure 15 illustrates his observations. Such an effect is significant in service if one considers that such overloads could correspond to operational interruptions or start-up.

Random loading tests conducted by Naumann (16), Schijve and DeRijk (17) and Barrois (18) have shown that crack propagation is a specific case of a quite general law on the behavior of notched specimens according to which any fatigue first improves the fatigue life under subsequent loads of lower level by creating beneficial residual compressive stresses at the notch roots subjected to tension.

2.3.8 Effect of Heat Treatment

It is not unexpected that heat treatment will affect the crack propagation rate and Maurin and Barrois (19), Schijve and DeRijk (20) and Broek (21) have demonstrated this. Maurin and Barrois' results for an AU2GN aluminum alloy are presented as Figure 16.

2.3.9 Effect of Environment

Considerable effort has been expended in evaluating the effects of the environment on the crack propagation rates. In general, aggressive environments induce higher crack propagation rates than inert; typical results by Hartman (20) are presented in Figure 17 wherein it is shown that the crack propagation rate is higher in distilled water than in dry air for an aluminum alloy. It should also be noted that an aggressive environment can induce crack propagation under a static load but this is beyond the scope of this thesis.

2.3.10 Effect of Strain Cycling

In the only such test, O'Neill (22) investigated the effect of strain cycling prior to the inducement of a fatigue crack. His results

(Figure 18) will be discussed in Chapter 4 in relation to the results observed by the author.

2.4 SUMMARY OF PREVIOUS WORK

As has been shown in the previous section, considerable effort has been expended in evaluating the effects of the many possible variables on the crack propagation rate in various materials. In summary, it has been determined that:

(a) The transition from the tensile to the shear mode of failure corresponds to a knee observed in the curve $\log \frac{da}{dN}$ vs ΔK.

(b) Following this transition, the crack propagation rate is proportional to a power of the alternating stress intensity factor.

(c) The type of load has no effect on the crack propagation rate; it is the alternating stress intensity factor which is important.

(d) The mean stress is of secondary importance compared to the alternating stress insofar as the crack propagation is concerned.

(e) The stress ratio $\sigma_{max}/\sigma_{min}$ is of little importance; it is the alternating stress $(\sigma_{max}-\sigma_{min})$ which is important.

(f) The crack propagation rate is inversely proportional to the cyclic frequency; the effect of frequency is, however, slight.

(g) Periodic overloading temporarily retards crack growth.

(h) The crack propagation rate is dependent upon the heat treatment of the material.

(i) An agressive environment will accelerate the crack growth rate.

3.0 EXPERIMENTAL PROGRAM

3.1 FORMULATION OF PROBLEM

In Chapter 2, a summary of previous studies done in the area of crack propagation was presented and it was shown that, while da/dN is governed to a large extent by the alternating stress intensity factor, the manner and condition of loading do have a secondary influence.

If the principles of fracture mechanics and crack propagation are to be applied with any confidence, the engineer must also know to what degree the material history prior to crack initiation will affect the subsequent crack growth. One such variable associated with the material history is strain cycling.

A component with a blunt stress raiser will withstand more strain cycling prior to crack initiation than will one with a sharp stress raiser. In addition, corrosion pits, nicks etc. may arise during service and will act as a stress raiser for crack initiation. In all instances the material will have undergone some degree of strain cycling (or fatigue damage) prior to the formation of the crack.

The present study was undertaken to investigate the effect of this fatigue damage on the subsequent crack propagation rate.

3.2 MATERIALS

The materials tested were two Alclad alloys (2024-T3 and 7075-T6) and one titanium alloy (Ti-6Al-4V). The mechanical properties are listed in Table 1 while Table 2 lists the chemical composition of each alloy. Both tables are based on the manufacturer's certified inspection reports.

3.3 PROCEDURE

The specimens were first subjected to a specific amount of fatigue damage by cycling at a constant stress amplitude to a number of cycles less than the endurance at the applied stress. A central through crack was then put in and the crack growth under a constant alternating load was monitored visually.

3.3.1 Prefatigue

Prefatigue was done using an Amsler High Frequency Vibrophore (shown in Figure 20); a two ton dynamometer was used for the aluminum specimens while a ten ton was used for the titanium. The material was machined to the shape shown in Figure 19a and subjected to stresses of 13400 ± 11840 psi and 29400 ± 26880 psi for the aluminum and titanium specimens respectively. These stresses were chosen such that failure would normally occur between 5×10^5 and 10^6 cycles. All cycling was done at a frequency of 110 cps. Emery cloth (#400 grit)was placed between the clamps and the specimens to alleviate fretting fatigue.

For each material, five specimens were cycled to approximately 90% of the endurance; for the 2024 alloy, a second series of five specimens were cycled to approximately 45% of tha endurance. For each material, five control specimens were prepared and left in the undamaged condition. Table 3 lists the specimens and the tests conducted.

3.3.2 Crack Growth Studies

Following the inducement of the fatigue damage, the specimens were modified to the shape shown in Figure 19b. The central crack was started by centrally drilling a 1/16 in diameter hole and making two fine saw cuts extending 1/8 in either side of the centerline.

Using a Gilmore Universal Closed Loop testing machine (shown in

Figure 21), the specimens were cycled at 6 cps. at a stress of 14578 ± 12889 psi and 17778 ± 16644 psi for the aluminum and titanium respectively. Once the crack was initiated on both sides, its growth was monitored visually using a Beck Vernier Microscope as shown in Figure 22.

3.4 RESULTS

The measured crack length vs. number of cycles are presented graphically as Figures AF-1 through AF-7 in Appendix A. Appendix A also lists the data in numerical form (Tables AT-1 through AT-7). The results were analyzed as detailed in Appendix B; a regression analysis was performed on the measured crack length vs. number of cycles and the resulting expression differentiated to evaluate the crack propagation rate da/dN. As trends only were sought, an approximate solution to the alternating stress intensity factor was made:

$$\Delta K = \Delta\sigma\sqrt{\ell} \qquad \text{(10)}$$

where $\ell = 2a$ = total crack length

The $d\ell/dN$ vs. ΔK data are presented as Appendix C.

4.0 OBSERVATIONS AND DISCUSSION OF RESULTS

4.1 CRACK LENGTH vs. NUMBER OF CYCLES

As a first approximation to evaluate the effect of fatigue damage on the crack growth rate, a comparison was made of the $d\ell/dN$ vs ΔK curves of the damaged with the undamaged specimens. The best comparison would be to statistically compare the mean curves from the lumped data at various values of N but considerably more data would be required to enable such an analysis to be representative. In the absence of such a statistical analysis, the author has compared the scatter bands of the individual tests. These are presented as Figures 23, 24 and 25 for the 2024, 7075 and titanium alloys respectively.

In Figure 23, a definite trend is observed towards a longer crack length for increasing prefatigue damage in the 2024-T3 aluminum alloy. No such trend is observed for either the 7075-T6 aluminum or the Ti-6Al-4V alloys.

Referring again to Figure 18, one observes that the author's results for the 2024-T3 tests appear to be in direct contradiction with O'Neill's. O'Neill, however, based his curves on two tests each and varied the stress as well as the number of cycles in prefatiguing his specimens. In any event, his results on the specimens damaged to 2×10^6 cycles fall very close to the undamaged and, had a greater number of tests been conducted, would probably have fallen within the scatter band of the undamaged.

4.2 CRACK PROPAGATION RATE vs. ALTERNATING STRESS INTENSITY FACTOR

The above comparison is, however, incomplete as the crack length in itself means little when it comes to design. A more meaningful comparison is made using the crack propagation rate and the alternating stress intensity factor in Figures 26, 27 and 28. Again, in the absence of a statistical analysis, the observed scatter bands have been compared.

As for the ℓ vs. N curves compared in the previous section, the $d\ell/dN$ vs. ΔK results show an effect of prior fatigue damage only for the 2024-T3 alloy. From Figure 26, the trend is toward a higher crack propagation rate for increasing fatigue damage. It will be noted that this effect is apparent only after the knee in the curve. As noted in §2.3.1, this knee corresponds to the transition from the flat tensile to the 45° shear failure. It was further observed by the author that specimen necking ahead of the crack tip was very pronounced for the 2024-T3 alloy following the transition to the shear failure mode; this necking was less apparent in the 7075 and titanium specimens.

4.3 DISCUSSION

The fact that the effect of prior fatigue damage was observed only in the 2024 aluminum alloy following the transition to the shear failure mode and that, of the three materials tested, this was the only material to exhibit necking ahead of the crack tip, suggests that ductility plays some role in this effect. From Table 1, the ratios of ultimate to yield strengths are 1.47, 1.10 and 1.02 for the 2024, 7075 and titanium alloys respectively. The elongations are respectively 19.0, 10.5 and

10.0%. These data show that, from the standpoint of ductility, the 2024 alloy clearly stands apart from the others.

5.0 CLOSURE

5.1 SUMMARY AND CONCLUSIONS

Three typical airframe materials (2024-T3 & 7075-T6 Alclad alloys and Ti-6Al-4V) in sheet form were subjected to fatigue damage by strain cycling at a constant amplitude to a number of cycles less than the endurance. The crack growth in these damaged specimens was compared to that in undamaged control specimens. The crack growth rate was evaluated by performing an exponential regression analysis on the observed data.

The comparison of the crack length and the crack growth rate of the damaged with the undamaged revealed a definite trend towards faster crack growth in the damaged 2024-T3 alloy; this effect was apparent only after the knee in the $d\ell/dN$ vs. ΔK curve. No such trend was observed in either the 7075 or titanium tests. It was noted that prior studies by Wilhem had established that this knee corresponds to the transition from the tensile to the shear mode of failure. It was further observed that only the 2024 specimens exhibited necking ahead of the crack tip and it was suggested that ductility played a major role in the effect of fatigue damage on the subsequent crack propogation rate.

5.2 SUGGESTIONS FOR FURTHER STUDY

Although a trend towards a deleterious effect of fatigue damage was observed in the more ductile material, further studies should be undertaken to evaluate this more fully. The author suggests that:

(1) The material evaluated by the author be retested in the same manner but that close attention be paid to the crack length at which the shear lips form.

(2) Using the author's results and the results from (1) above, a statistical analysis be applied to the $d\ell/dN$ vs. ΔK results.

(3) The effect of ductility be further evaluated by conducting crack propagation studies on materials heat treated to varying degrees of hardness.

The experience gained by the author has also shown the need for the development of a device which would continuously monitor the crack growth; it is also desirable that such a monitor be able to differentiate between the tensile and the shear failure modes. It is the author's opinion that ultrasonics would be best suited to this purpose.

It should be further noted that, although a considerable amount of work has been done investigating the effects of the many possible variables, further work is required in order to clarify their effects. A detailed program should be undertaken to evaluate and tabulate the design factors associated with these variables.

6.0 REFERENCES

1. Barrois W. Manual on Fatigue of Structures
   AGARD-MAN-8-70, June 1970
2. Griffith A. The Phenomenon of Rupture and Flow in Solids
   Phil. Trans. Roy. Soc. (London), Series A
   V 221, 1920, pp163-198
3. Irwin G. Fracture, Encyclopedia of Physics
   V 6, 1958, p551
4. Isida M. Stress Concentration at the Tip of a Central Transverse
   Itaki Y. Crack in a Stiffened Plate Subjected to Tension
   Proc. 4th U.S. Nat.Cong. of Appl. Mech.
   Berkley, Calif, V II, June 1962
5. Baharandi S. Thèse, Ecole Nationale Supèrieur de l'Aeronautique
   Paris, 1969
6. Wilhem D. Investigation of Cyclic Crack Growth Transitional Behavior
   Fatigue Crack Propagation, ASTM STP 415, 1967
7. Donaldson Crack Propagation Behavior of Some Airframe Materials
   Anderson Crack Propagation Symposium, Cranfield, 1961
8. Paris P. Proceedings of 10th Sagamore Arm Materials Research
   Conference - Syracuse Univ. Press, 1965
9. Frost Fatigue Tests on Notched Mild Steel Plates with Measurements
   Dugdale of Fatigue Cracks - J. Mech. Phys. Solids
   V 5 No 3, p181, 1956
10. Broek Influence of Mean Stress on Propagation of Fatigue Cracks
    Schijve in Aluminum Alloy Sheet - NLR TN-M2111, Amsterdam, Jan. 1963
11. Lehr Fatigue Crack Propagation and Strain Cycling Properties
    Liu Int. Jour. of Fracture Mechanics, V 5 No. 1, p45, March 1969

12. Hartman et al — Some Tests on the Effect of Environment on the Propagation of Fatigue Cracks in Aluminum Alloy Sheet
NLR TN-M2182, May 1967

13. Schijve J. et al — The Effect of the Frequency of an Alternating Load on the Crack Rate in a Light Alloy Sheet
NLR TN-M2092, Amsterdam, Sept. 1961

14. Illg W. McEvily A. — The Rate of Fatigue Crack Propagation for Two Aluminum Alloys Under Completely Reversed Loading
NASA TN D-52, Oct. 1959

15. Schijve J. — Fatigue Crack Propagation in Light Alloy Sheet Material and Structures - NLL Report MP 195, Amsterdam, 1960

16. Naumann E. — Evaluation of the Influence of Load Randomization and of Ground-Air-Ground Cycles on Fatigue Life
NASA TN D-1584, Oct. 1964

17. Schijve J. de Rijk P. — The Effect of Ground to Air Cycles on the Fatigue Crack Propagation in 2024-T3 Alclad Sheet Material
NLR TR-M2148, July 1966

18. Barrois W. — Les Essais Statiques et de Fatigue des Structures d'Avions en France et à l'Etranger
Doc. Air. Espace No 110, p16, Paris, May 1968

19. Maurin E. Barrois W. — Influence de la Fréquence et de la Température d'Essai sur la Durée en Fatigue d'Eprouvettes et d'Assemblages en Tôle A-U2GN-T6 - l'Aéronautique et l'Astronautique
No 9, Paris, 1969

20. Schijve J. de Rijk P. — Fatigue Crack Propagation in 2024-T3 Alclad Sheet Materials From Seven Different Manufacturers
NLR TR-M2162, May 1966

21. Broek D. Crack Propagation Properties of 2024-T8 Sheet Under Static and Dynamic Loads - NLR TM-M2161, March 1966

22. O'Neill P. Effect of Prior Fatigue Loading on Crack Propagation Rates in 2024-T3 Sheets - RAE Tech. Rept. 66100, March 1966

23. Tiffany Applied Fracture Mechanics
Masters Fracture Toughness Testing And Its Applications
ASTM STP 381, p249, 1965

24. Paris Stress Analysis of Cracks
Sih Fracture Toughness Testing And Its Applications
ASTM STP 381, p30, 1965

25. Schijve J. Fatigue Crack Propagation in Unnotched and Notched
Jacobs F. Aluminum Alloy Specimens - NLR TR-M2128, May 1964

26. Weibull W. Size Effect on Fatigue Crack Initiation
FFA Report 86, Stockholm, 1960

27. Weibull W. The Effect of Size and Stress History on Fatigue Crack Propagation - Crack Propagation Symposium, Cranfield 1961

28. Hudson C. The Effect of Changing Stress Amplitude on the Rate of Fatigue Crack Propagation in Two Aluminum Alloys
NASA TN D-960, Sept. 1961

29. Frost N. The Fatigue Crack Propagation Characteristics of
Denton K. Titanium and Two Titanium Alloys
Metallurgia, Sept. 1964, p113

30. Schijve J. The Effect of Sheet Width on the Fatigue Crack Propagation
et al in 2024-T3 Alclad Material - NLR TR-M2142, 1965

31. Broek D. The Transition of Fatigue Cracks in Alclad Sheet
et al NLR TR M2100, Nov. 1962

32. Schijve J. The Effect of Temperature and Frequency on the Fatigue
de Rijk P. Crack Propagation in 2024-T3 Alclad Sheet Material
NLR TR-M2138, Jan. 1965

33. Broek D. The Effect of Heat Treatment on the Propagation of
et al Fatigue Cracks in Light Alloy Sheet Material
NLR TR-M2134, May 1963

34. Hartman A. The Effect of Environment and Load Frequency on the Crack
Schijve J. Propagation Law for Macro Fatigue Crack Growth in Aluminum
Alloys - NLR MP-69001, April 1968

35. Barsom J. Investigation of Subcritical Crack Propagation
Ph.D. Thesis, U. of Pittsburgh, 1969

36. Forman R. Numerical Analysis of Crack Propagation in Cyclic
et al Loaded Structures - J. Basic Engr., Trans. ASME, 1967, p459

37. Hahn G. Local Yielding and Extension of a Crack Under Plane Stress
Rosenfield A. Acta Metallurgia, v 13, Mar. 1965, p293

38. Irwin G. Analytical Aspects of Crack Stress Field Problems
Dept. of Theo. & Appl. Mech., U. of Illinois
T. & A. M. Report 213

39. Johnson Sub-Critical Flaw Growth
Paris J. of Engr. Fract. Mech., V 1, No 1, 1968, p3

40. Liu N. Crack Propagation in Thin Metal Sheet Under Repeated
Loading - J. of Basic Engr., Trans. ASME, Mar. 1961, p23

41. Lambert The Importance of Service Inspections in Aircraft Fatigue
Aircraft Engineering, October, 1967

42. Wei R. Fatigue Crack Propagation in a High Strength Aluminum
Alloy - Int. J. of Fract. Mech., V 4, No 2, June 1968, p159

43. McEvily A. Illg W. The Rate of Fatigue Crack Propagation in Two Aluminum Alloys - NACA TN 4394, Sept. 1958

44. Wei R. et al Fatigue Crack Propagation in Some Ultra High Strength Steels - ASME Paper 66-MET-3, Apr. 1966

45. Hudson C. Fatigue Crack Propagation in Several Titanium and Stainless Steel Alloys and One Superalloy NASA TN D-2331, Oct. 1964

TABLE 1 MECHANICAL PROPERTIES

A. Aluminum Alloys (Alclad)

Type	No of Tests	UTS (ksi)		2% YS (ksi)		Elongation(%)	
		Max.	Min.	Max.	Min.	Max.	Min.
2024 T3	6	62.7	62.1	44.0	40.8	19.0	16.5
7075 T6	4	78.0	76.7	71.4	69.2	10.5	10.0

B. Titanium Alloy (Annealed & Pickled)

Type	Hard-ness	UTS (ksi)		2% YS (ksi)		Elongation(%)	
		L	T	L	T	L	T
Ti-6Al-4V	R_C-36	169.6	150.0	165.5	132.1	10.0	9.0

TABLE 2 CHEMICAL COMPOSITION

A. Aluminum Alloys

Type	Si		Fe	Cu		Mn		Cr		Zn		Mg		Ti	Other	
	Max	Min	Max	Max	Min	Max	Min	Max	Min	Max	Min	Max	Min	Max	Ea.	Tot.
2024 T3	.50	-	.50	4.9	3.8	0.9	0.3	0.1	-	.25	-	1.8	1.2	-	.05	.15
7075 T6	.50	-	.70	2.0	1.2	0.3	-	0.4	.18	6.1	5.1	2.9	2.1	.20	.05	.15

B. Titaniun Alloy

Type	C	Fe	N	H	O	V	Al
Ti-6Al-4V	0.025	0.14	0.12	65ppm	0.16	4.2	6.45

TABLE 3 SPECIMEN IDENTIFICATION

Condition	2024 T3	7075 T6	Ti-6Al-4V
Undamaged	24-1 thru 5	75-1 thru 5	Ti-1 thru 4
45% damage	24-6 thru 10	-	-
90% damage	24-11 thru 15	75-6 thru 10	Ti-5 thru 9

FIGURES

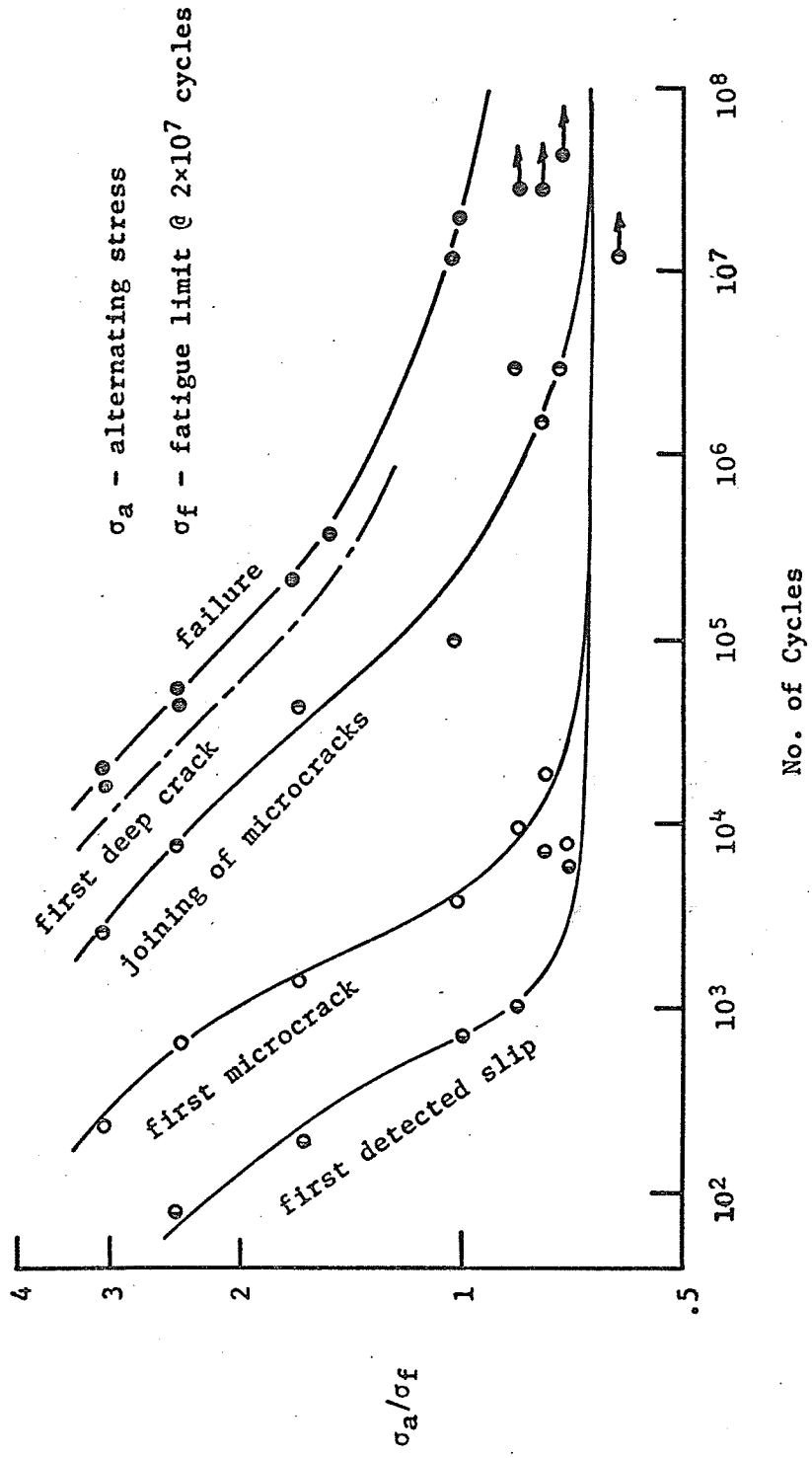

FIGURE 1

STAGES IN FATIGUE FAILURE (1)

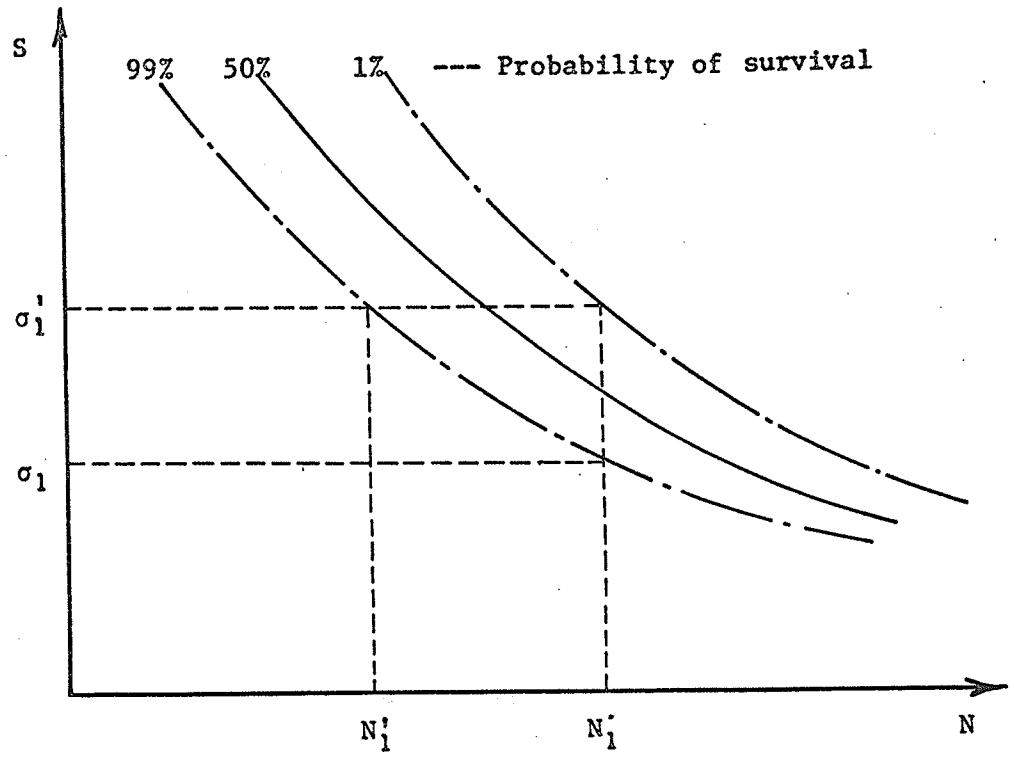

FIGURE 2

TYPICAL S-N CURVE

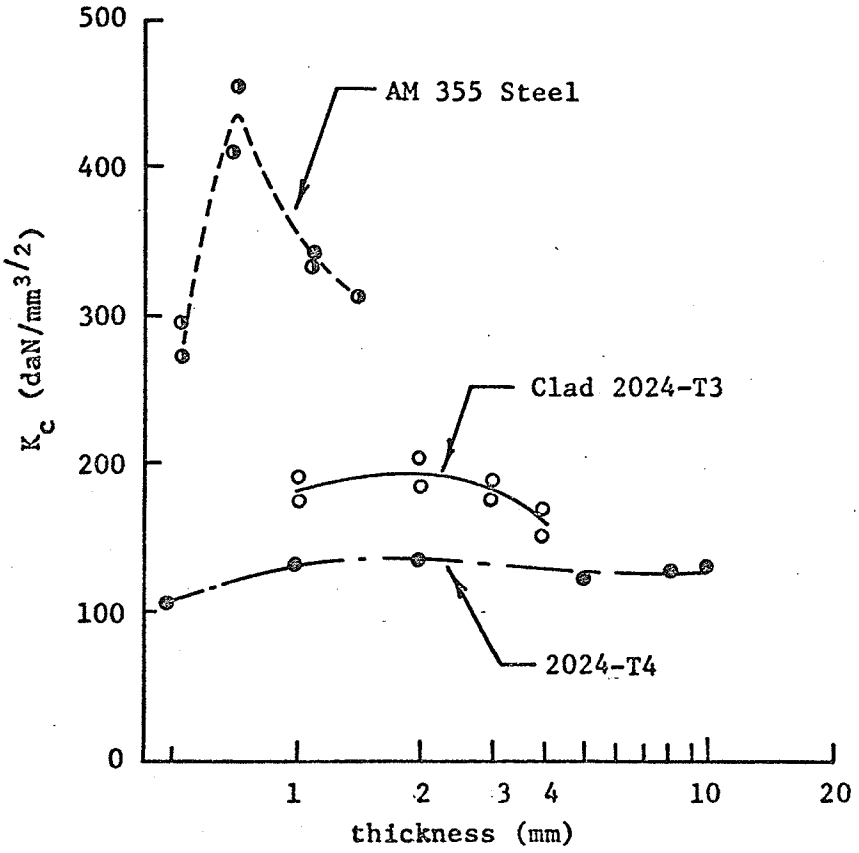

FIGURE 3

K_c DEPENDENCE ON THICKNESS (1)

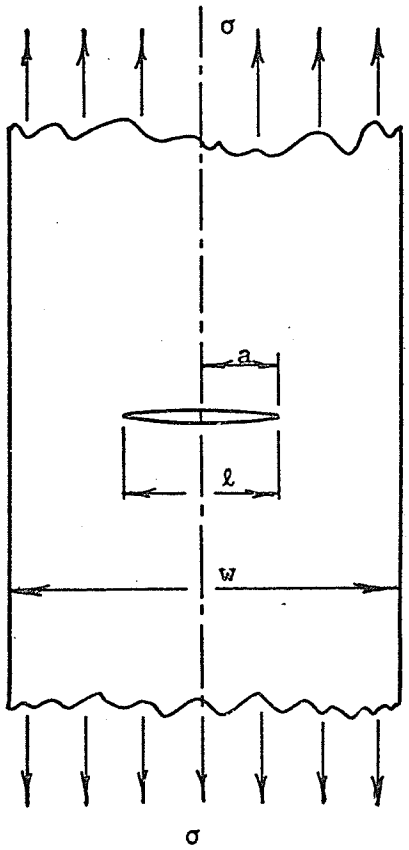

FIGURE 4

FINITE WIDTH SHEET
WITH CENTRAL THROUGH CRACK

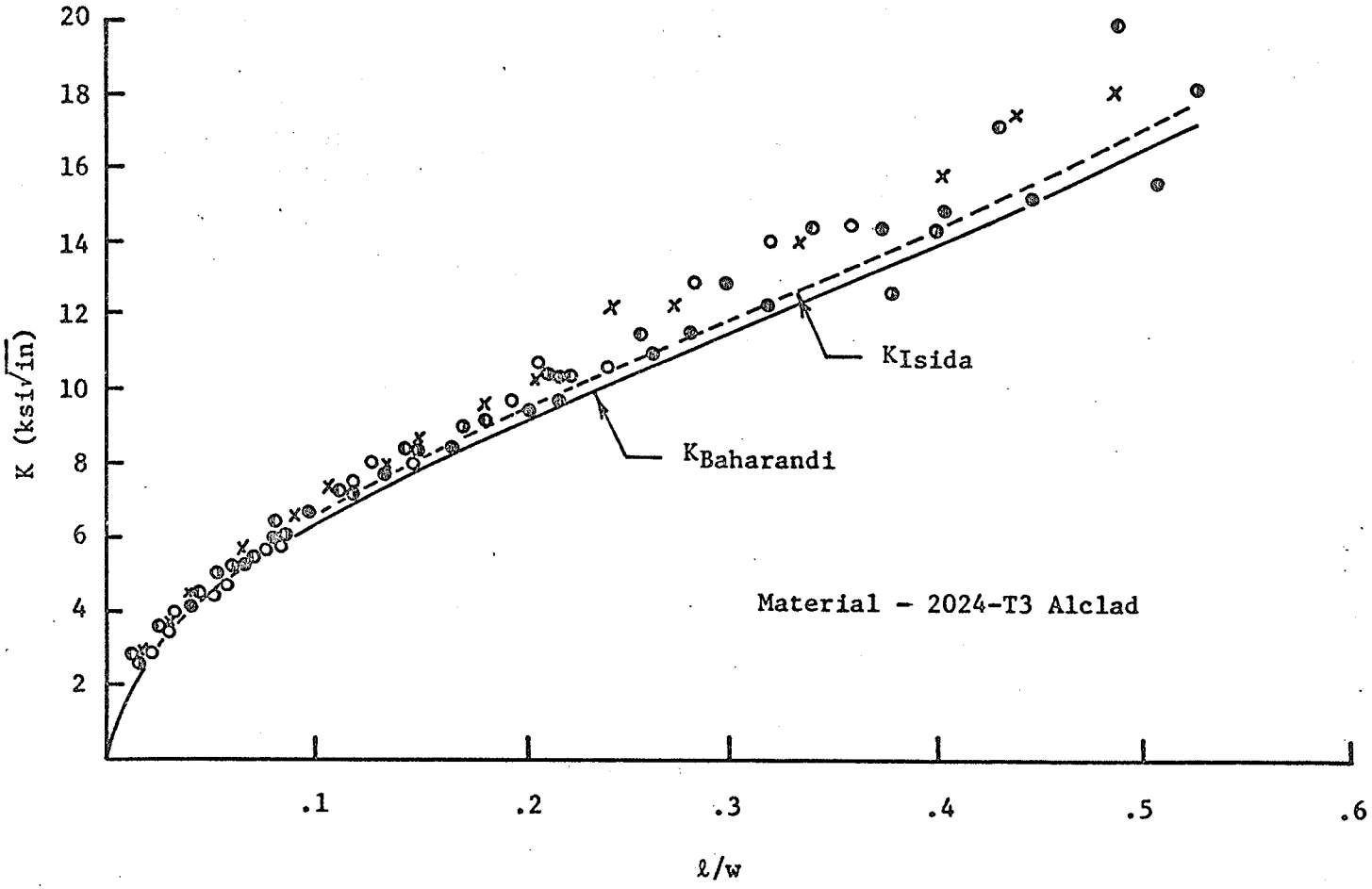

FIGURE 5

EXPERIMENTAL vs. THEORETICAL STRESS INTENSITY FACTOR (5)

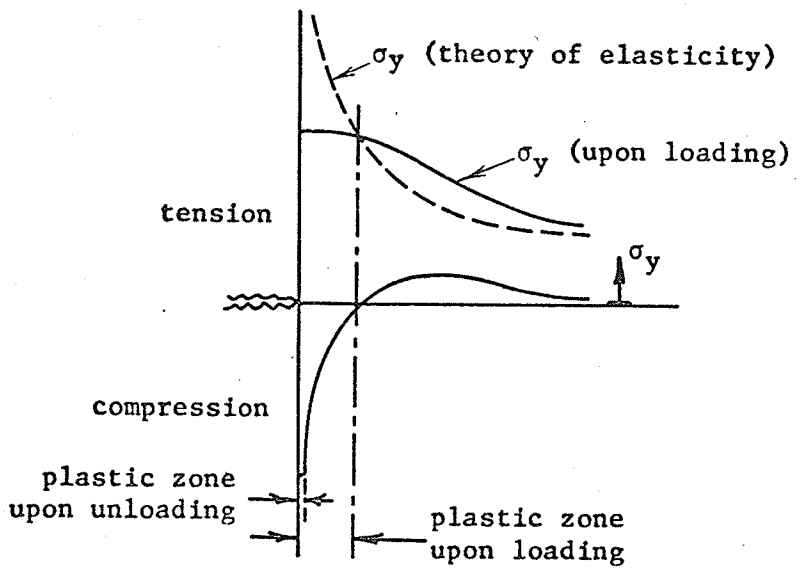

FIGURE 6

CRACK TIP STRESS DISTRIBUTION

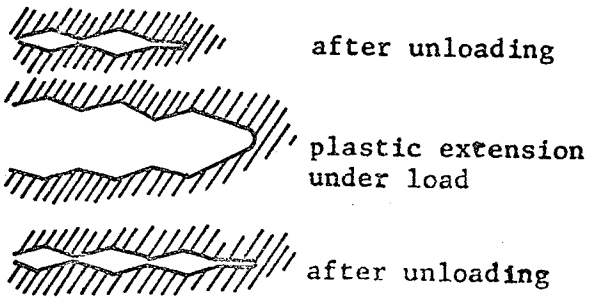

FIGURE 7

FATIGUE CRACK GROWTH

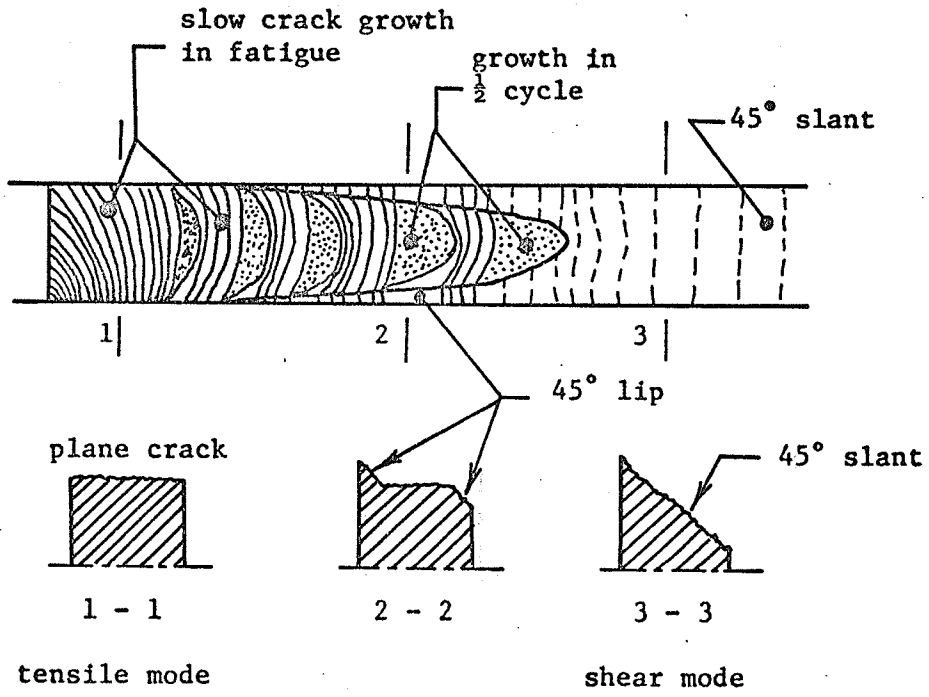

FIGURE 8

TRANSITION FROM TENSILE TO SHEAR MODE

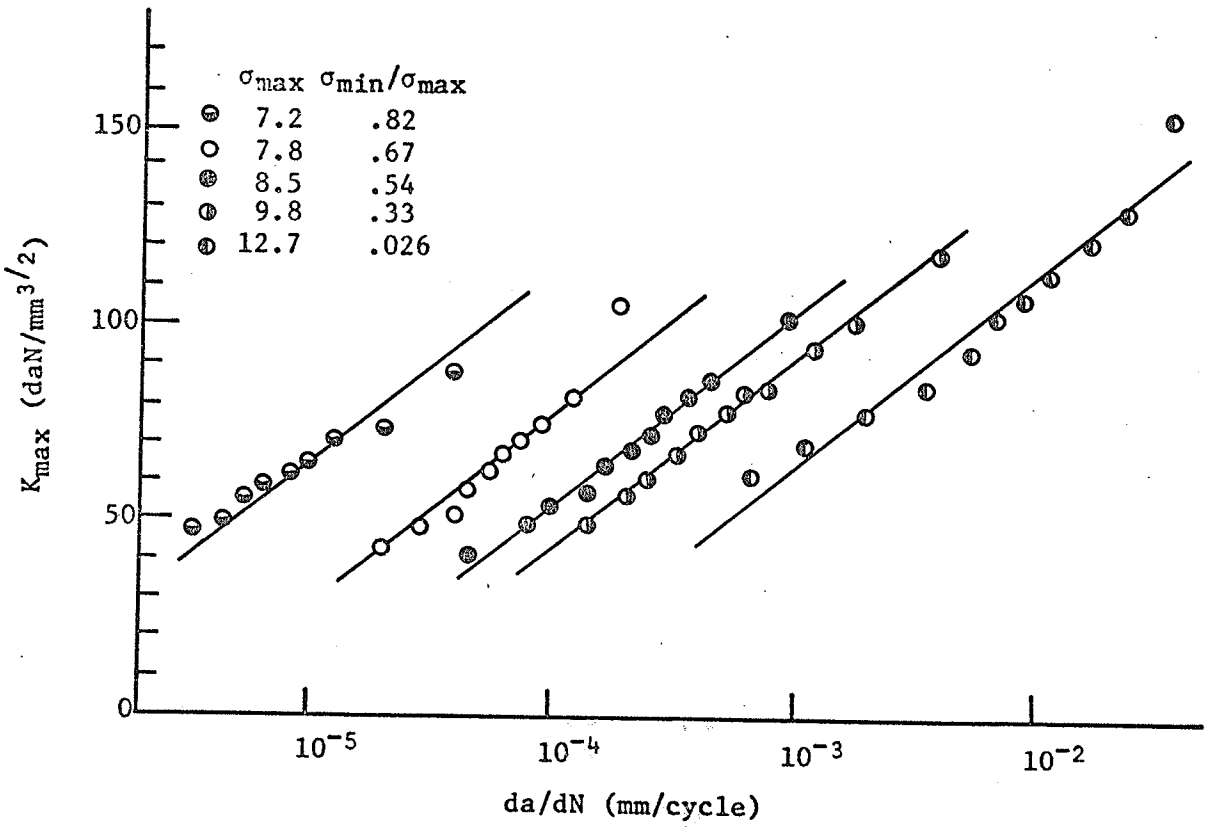

FIGURE 9

da/dN vs. K_{max} FOR 2024-T3 (6)

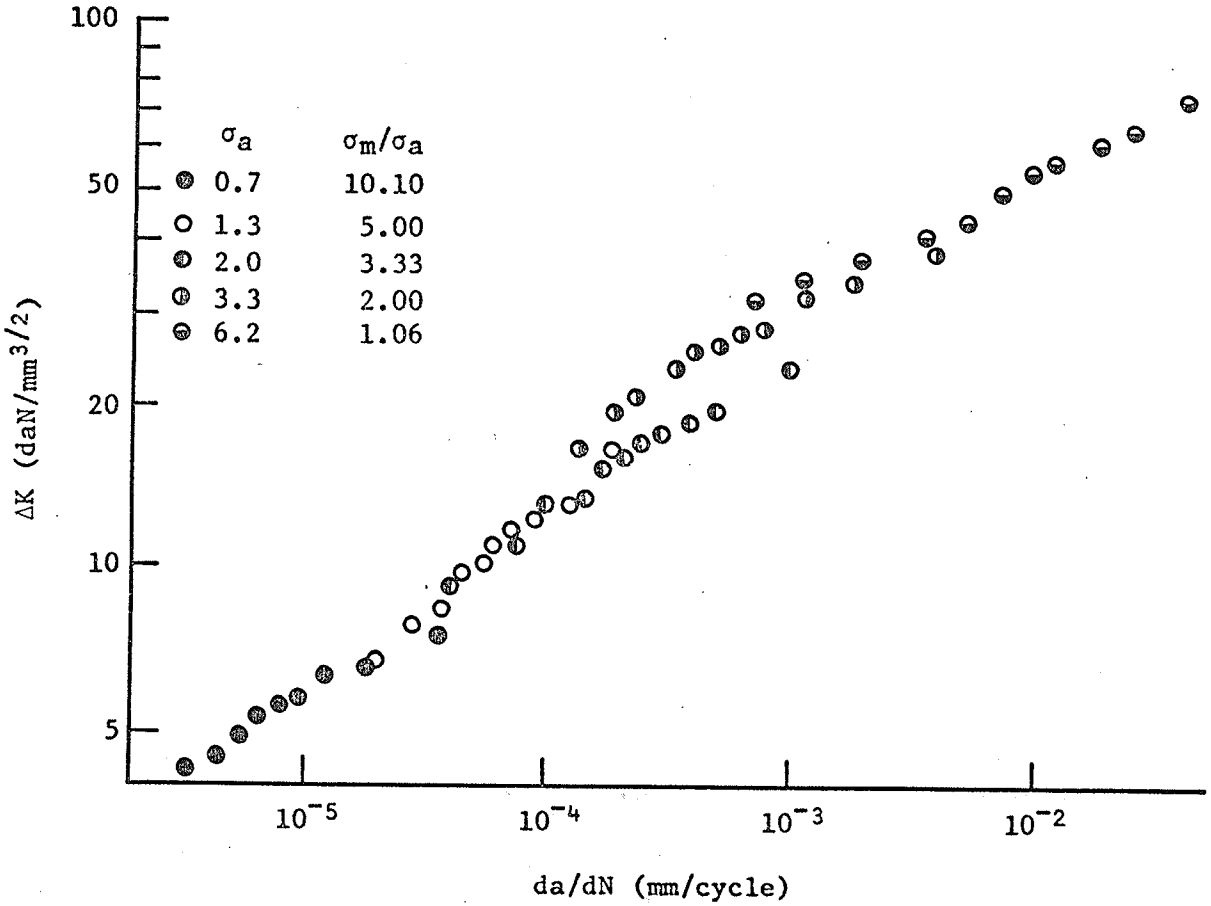

FIGURE 10

da/dN vs ΔK FOR 2024-T3 (6)

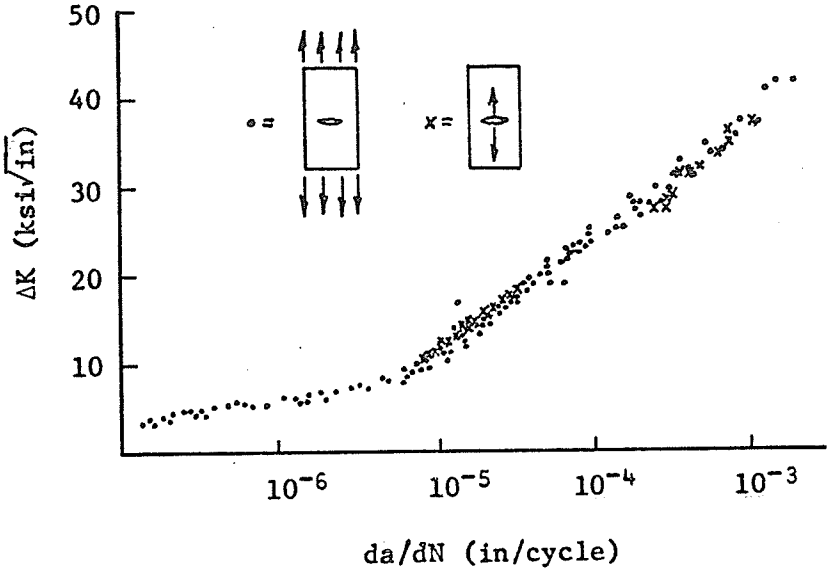

FIGURE 11

EFFECT OF LOAD TYPE ON 2024-T3 (7)

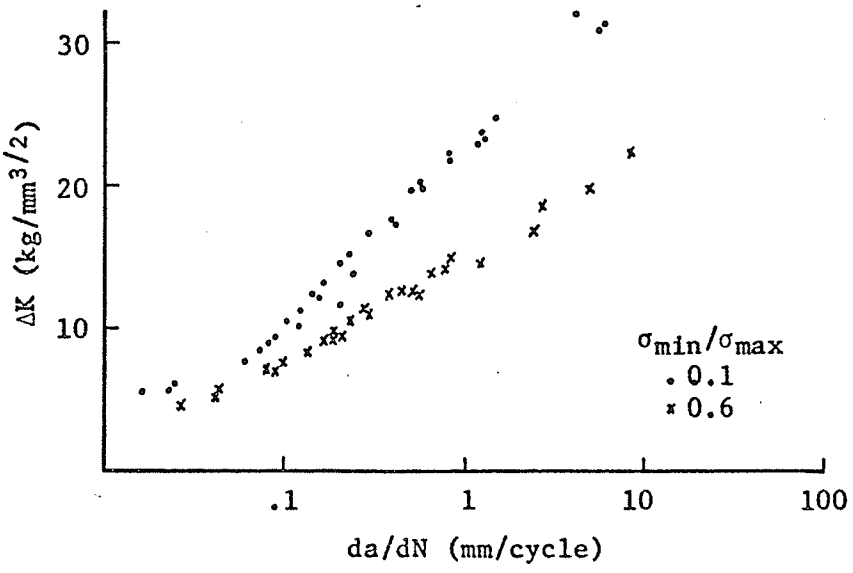

FIGURE 12

EFFECT OF STRESS RATIO ON 2024-T3 (9)

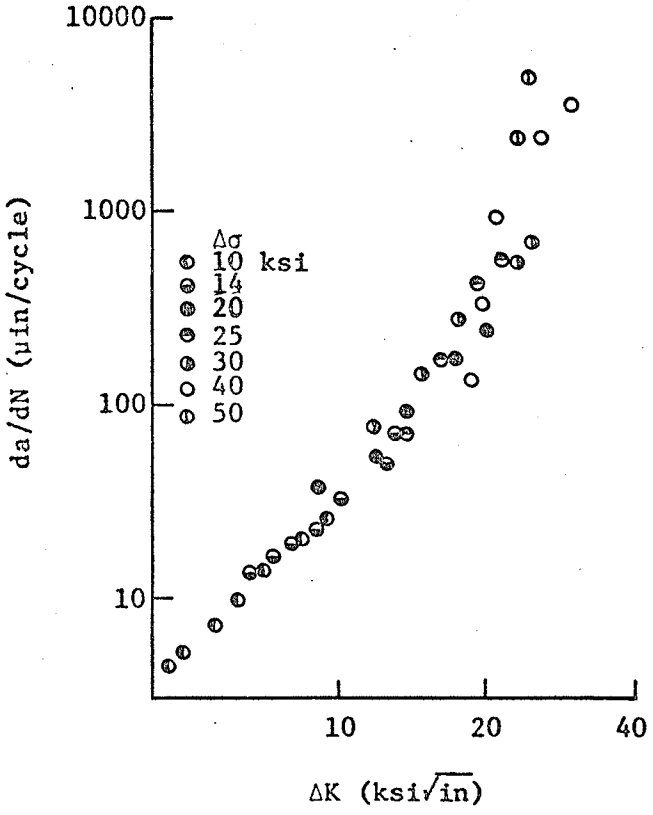

(a) 2024-T4

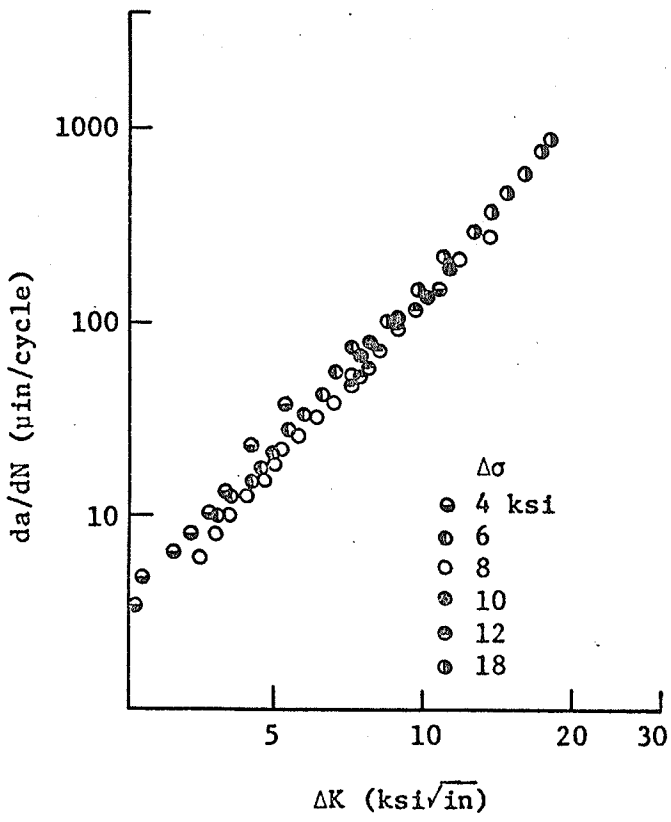

(b) 7075-T6

FIGURE 13

EFFECT OF STRESS RANGE
ON TWO ALUMINUM ALLOYS (10,42)

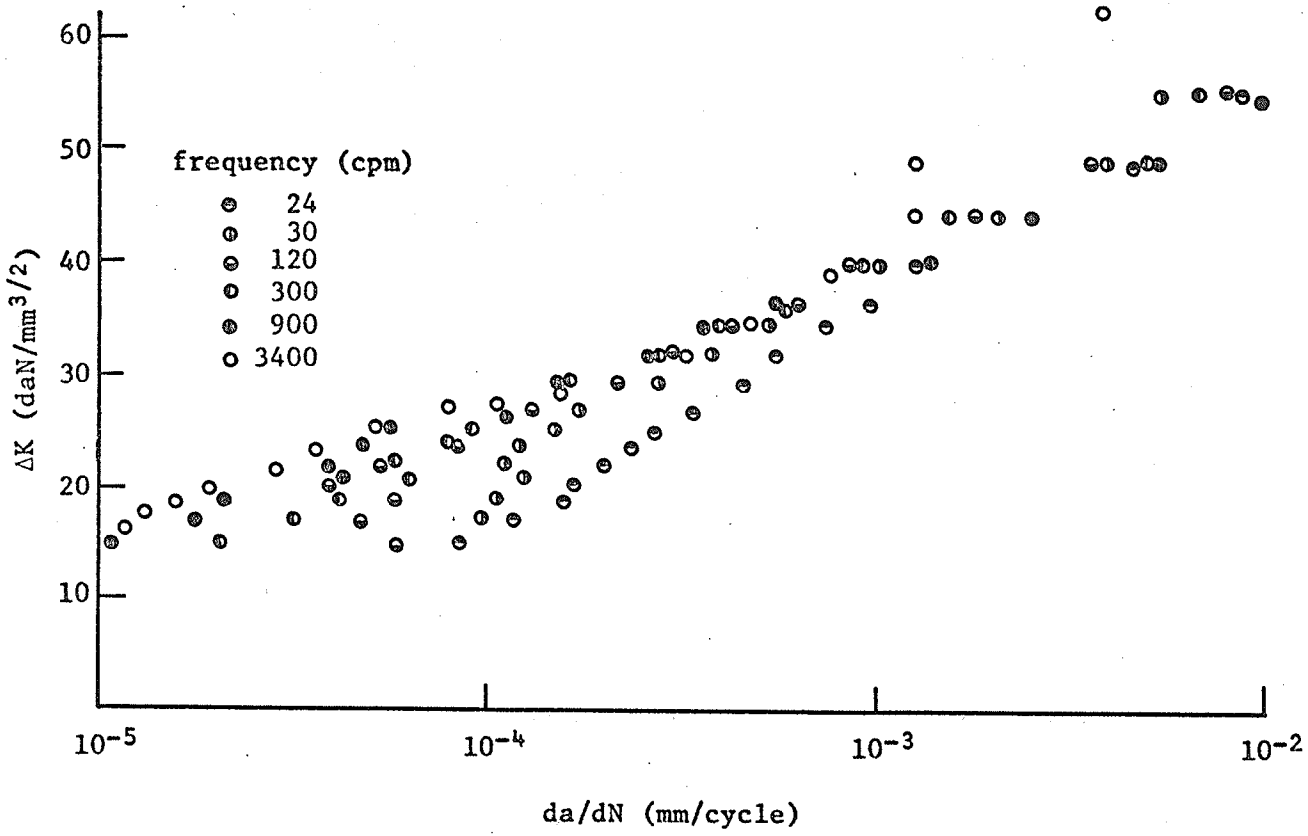

FIGURE 14

EFFECT OF FREQUENCY ON 2024-T3 (11)

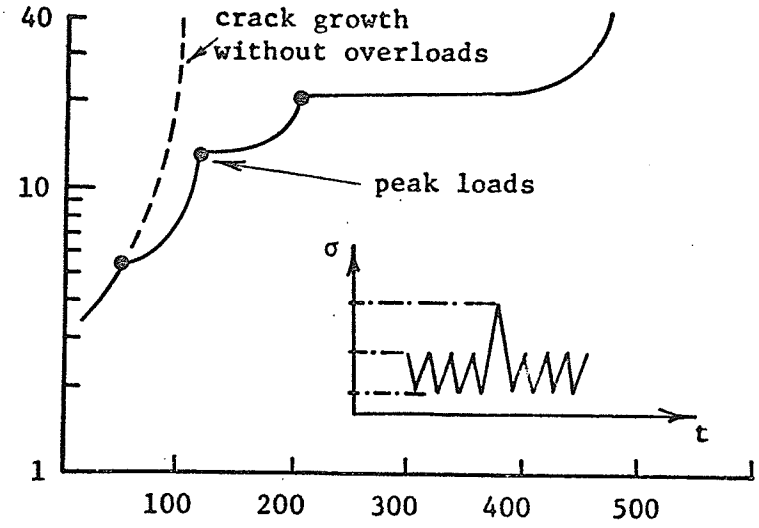

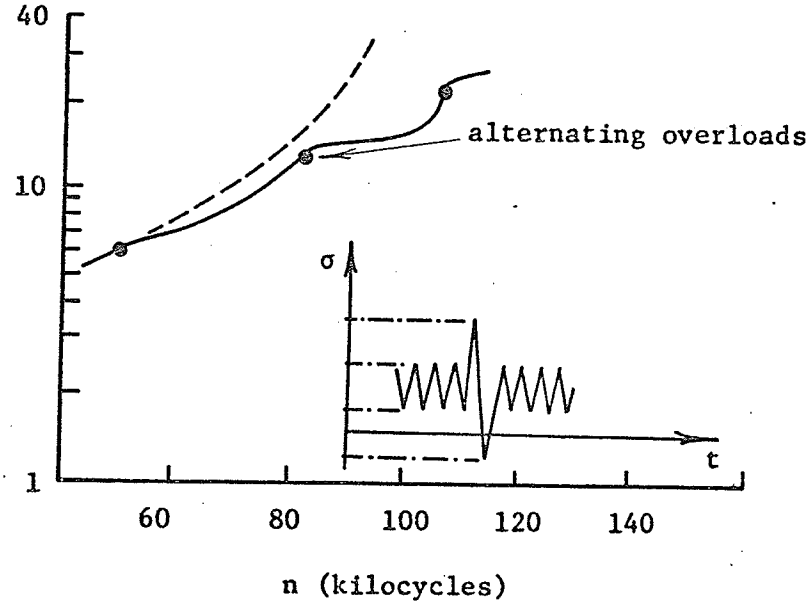

FIGURE 15

EFFECT OF OVERLOADING ON 2024 SHEET (14)

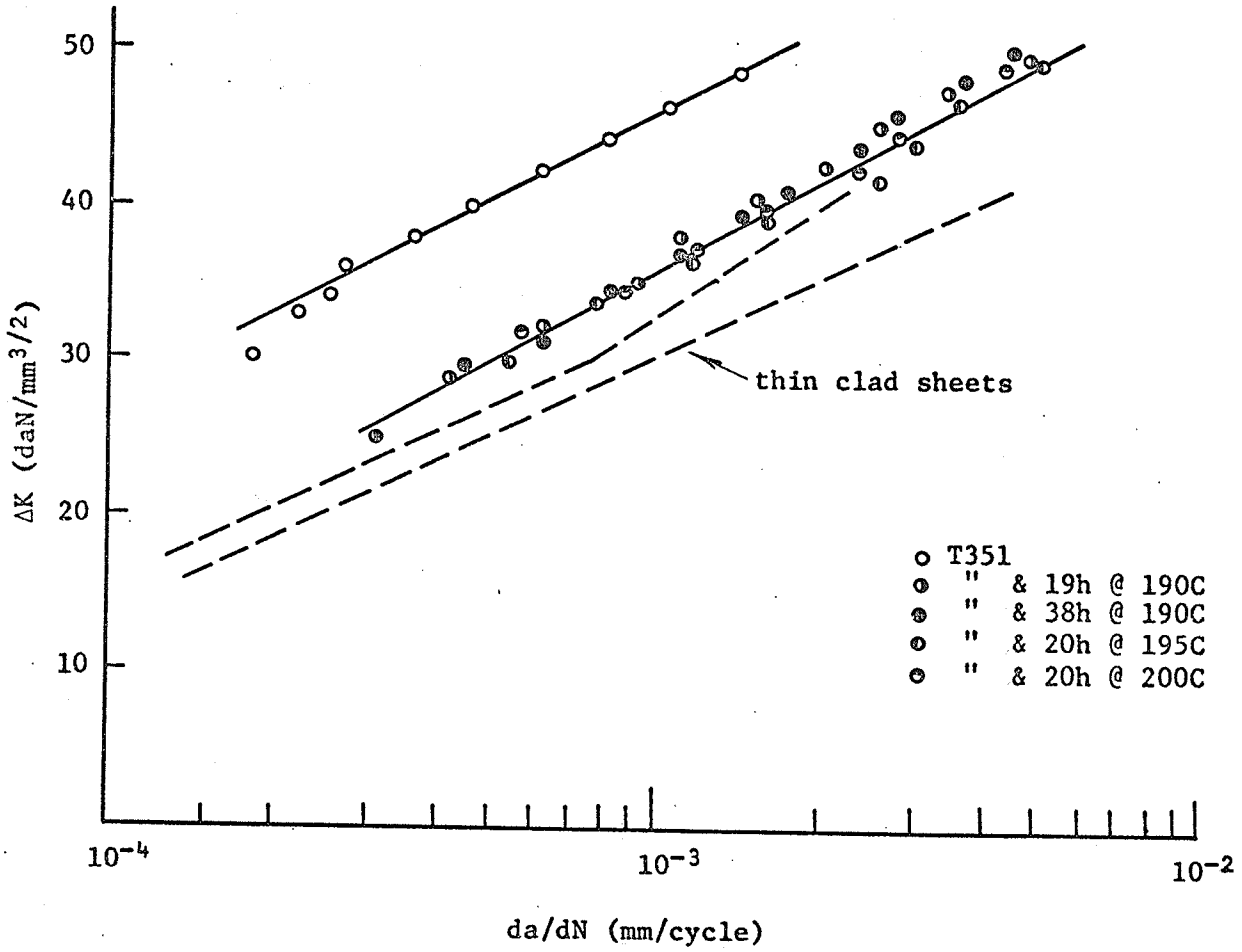

FIGURE 16

EFFECT OF HEAT TREATMENT
ON A-U2-GN PLATES (18)

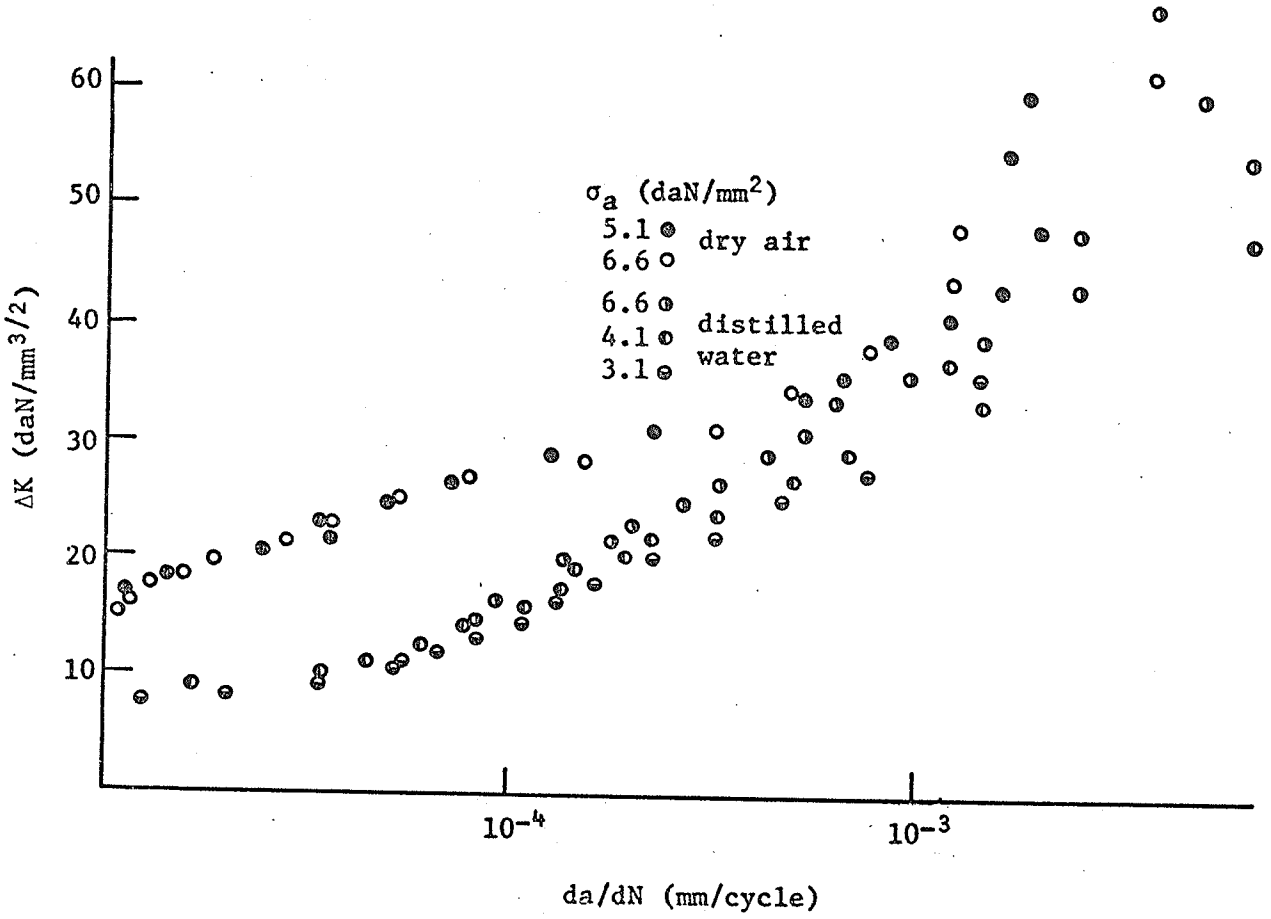

FIGURE 17

EFFECT OF ENVIRONMENT ON 2024-T3 (19)

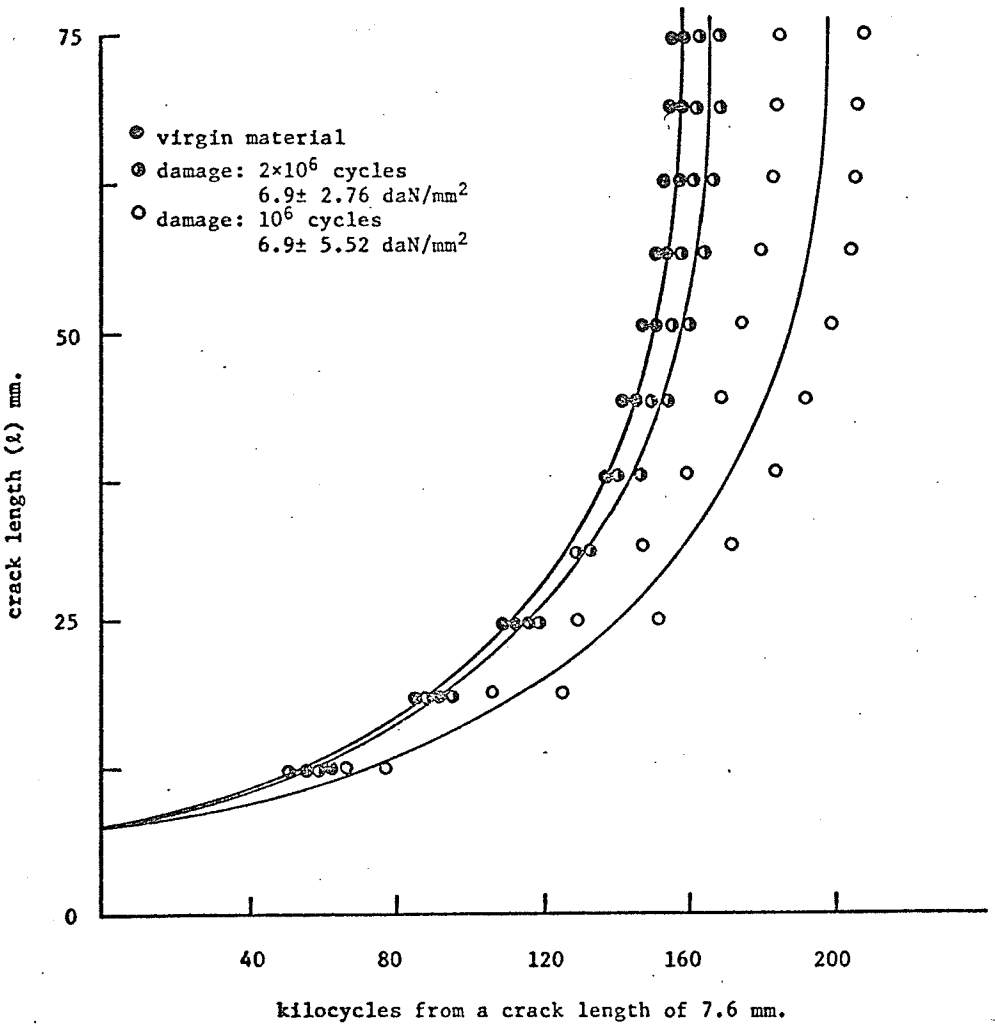

FIGURE 18

EFFECT OF PRIOR FATIGUE ON 2024-T3 (20)

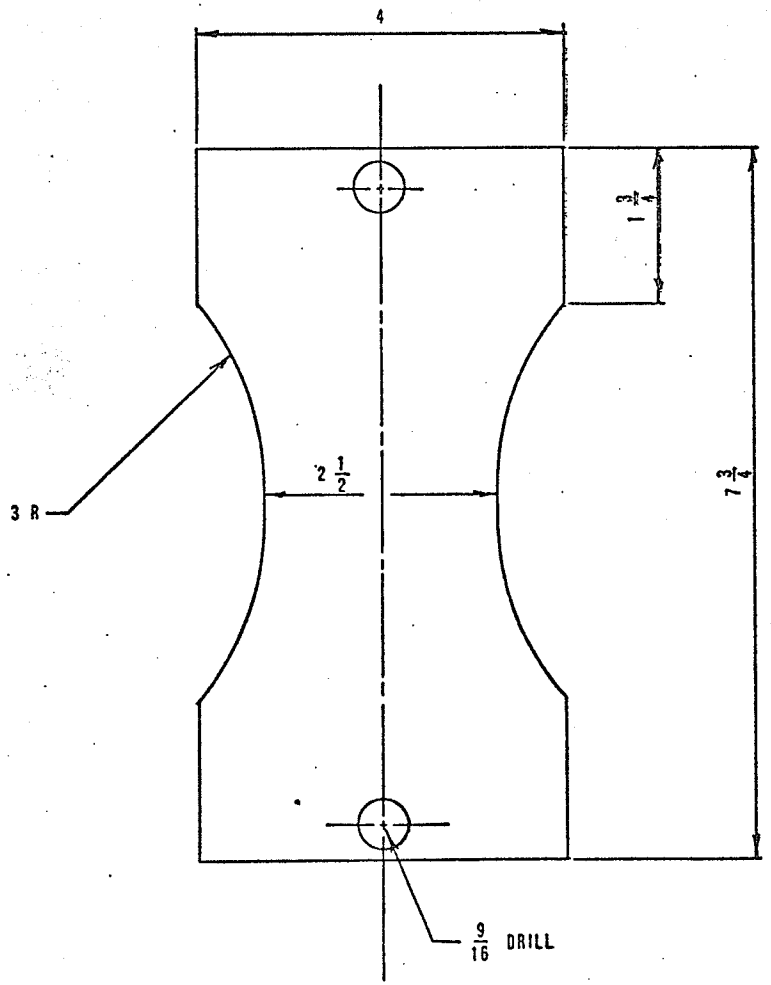

(a) Prefatigue

Specimen Thickness: Aluminum .050"

Titanium .0625"

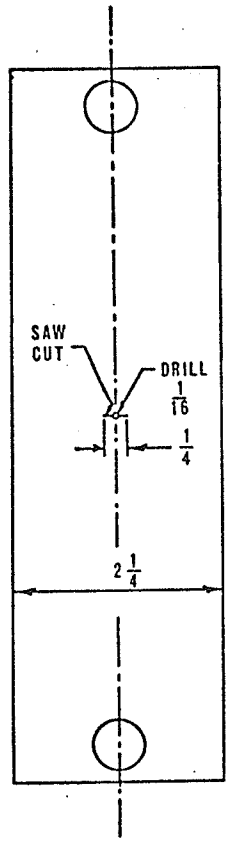

(b) Crack Growth

FIGURE 19

SPECIMEN GEOMETRY

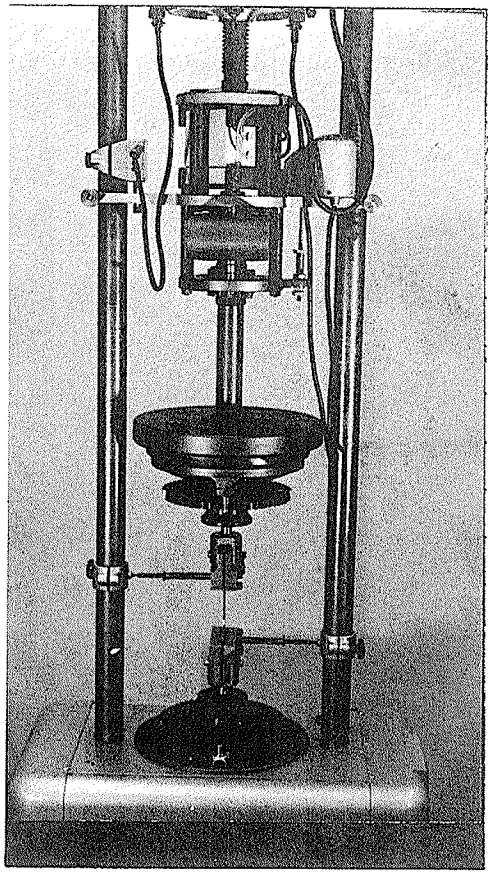

View A

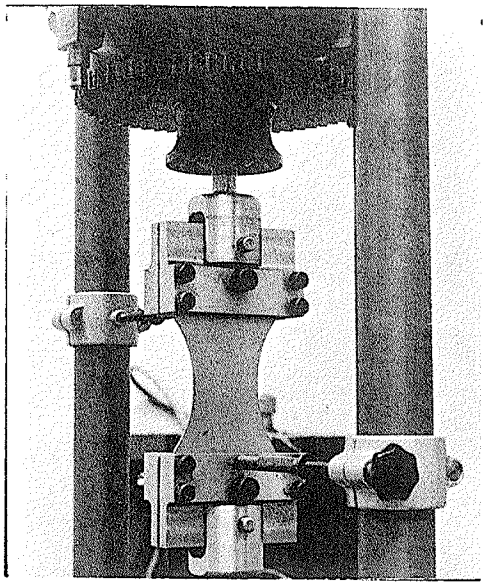

Specimen

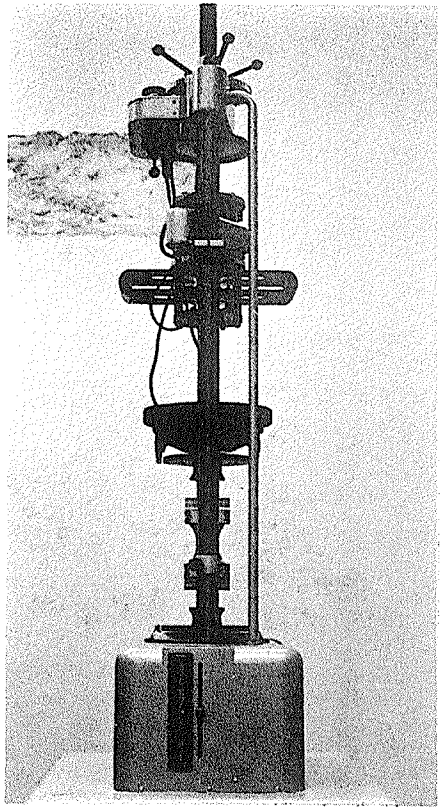

View B

FIGURE 20

AMSLER HIGH FREQUENCY VIBROPHORE

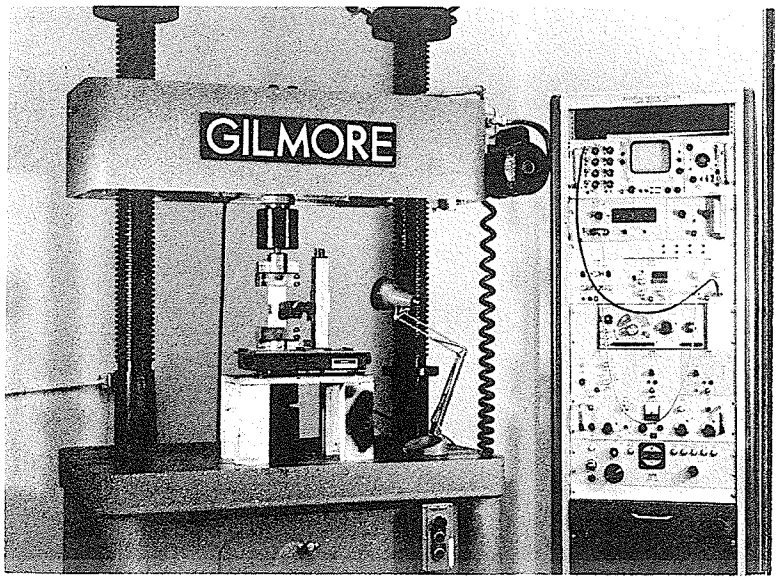

FIGURE 21

GILMORE TESTING MACHINE

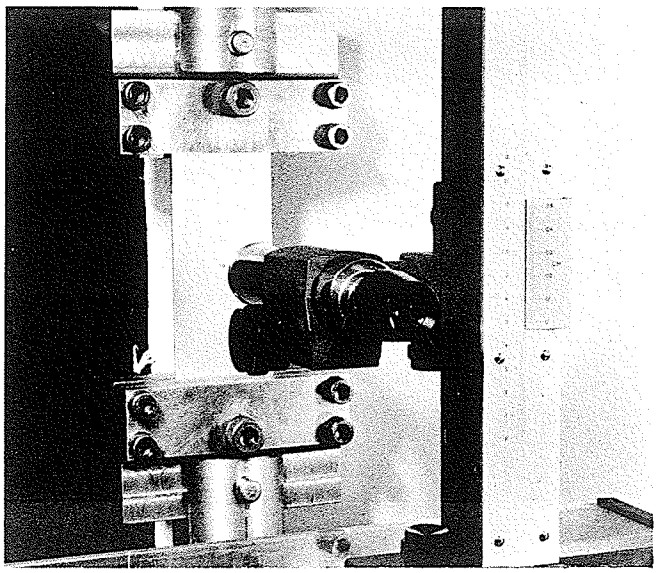

FIGURE 22

MEASUREMENT TECHNIQUE

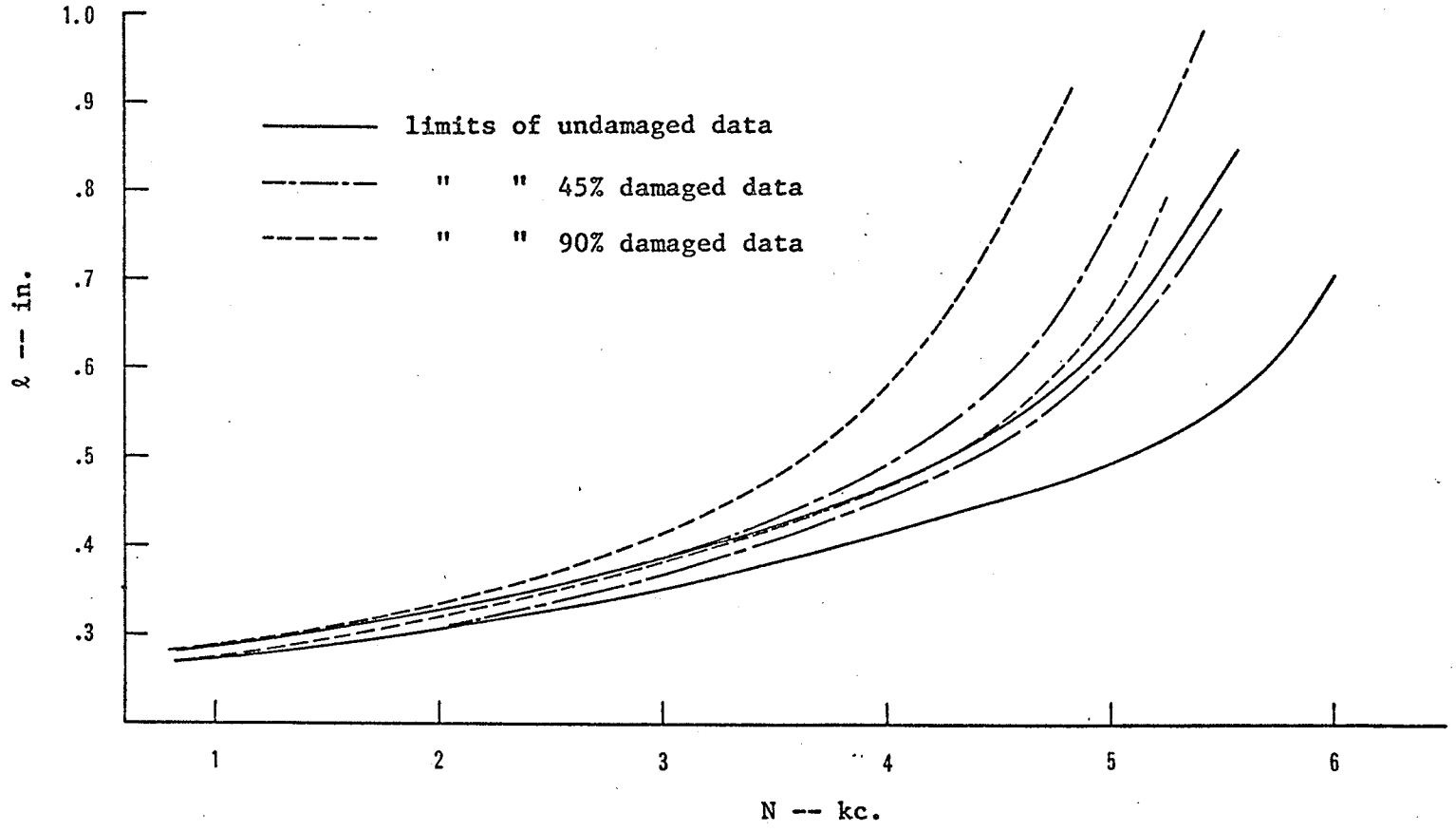

FIGURE 23

2024-T3 ℓ vs N SCATTER

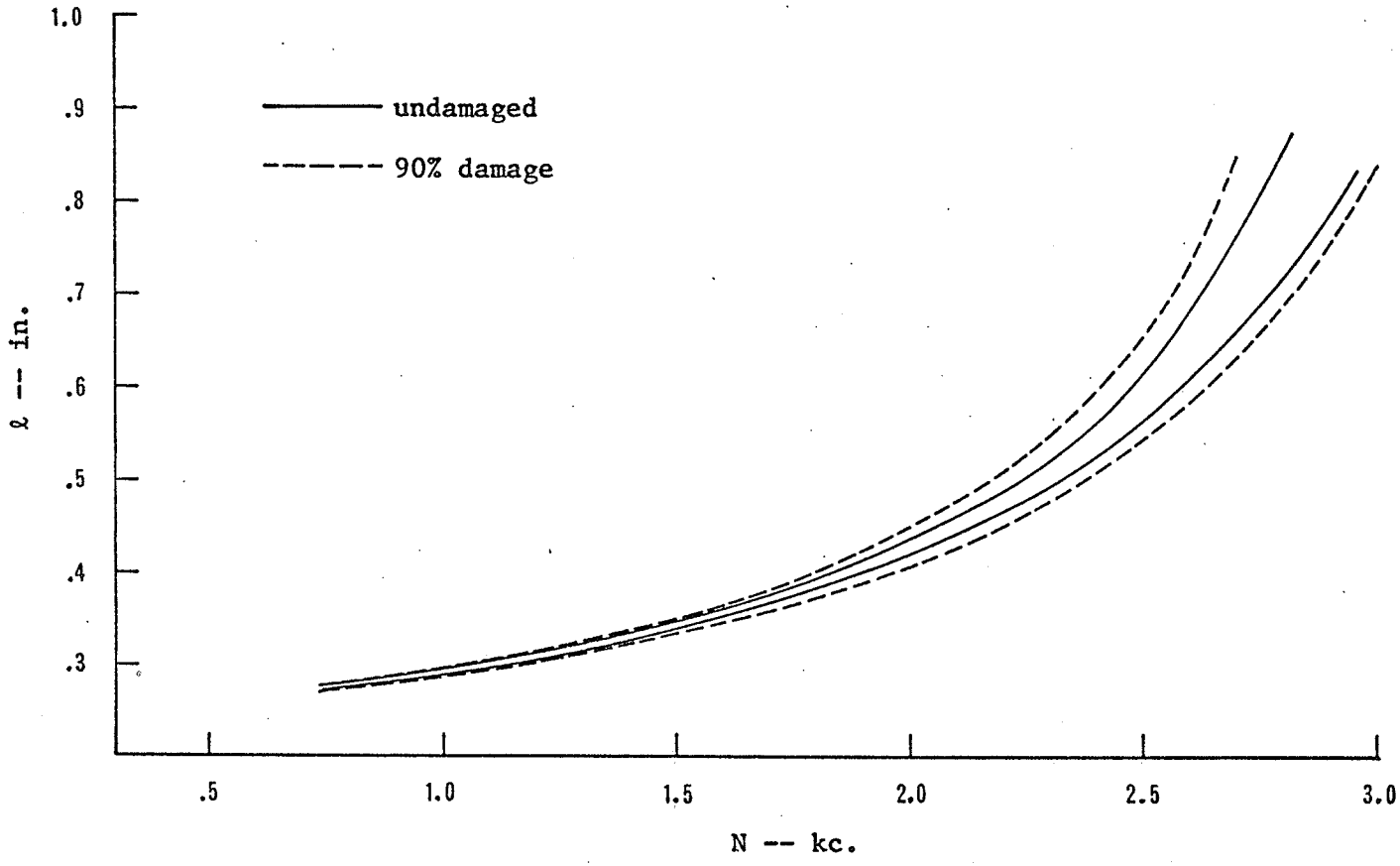

FIGURE 24

7075-T6 ℓ vs N SCATTER

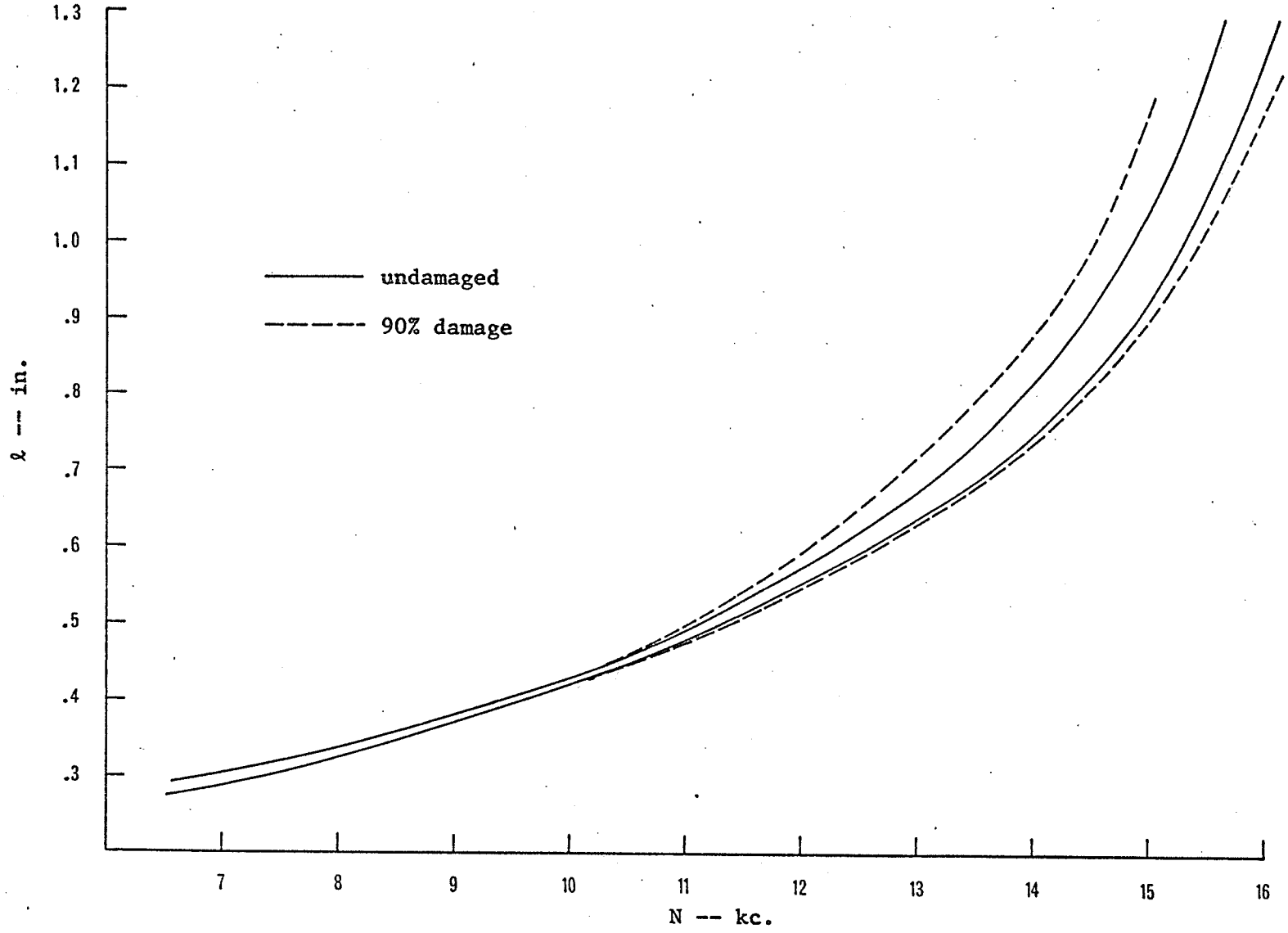

FIGURE 25

Ti-6Al-4V ℓ vs N SCATTER

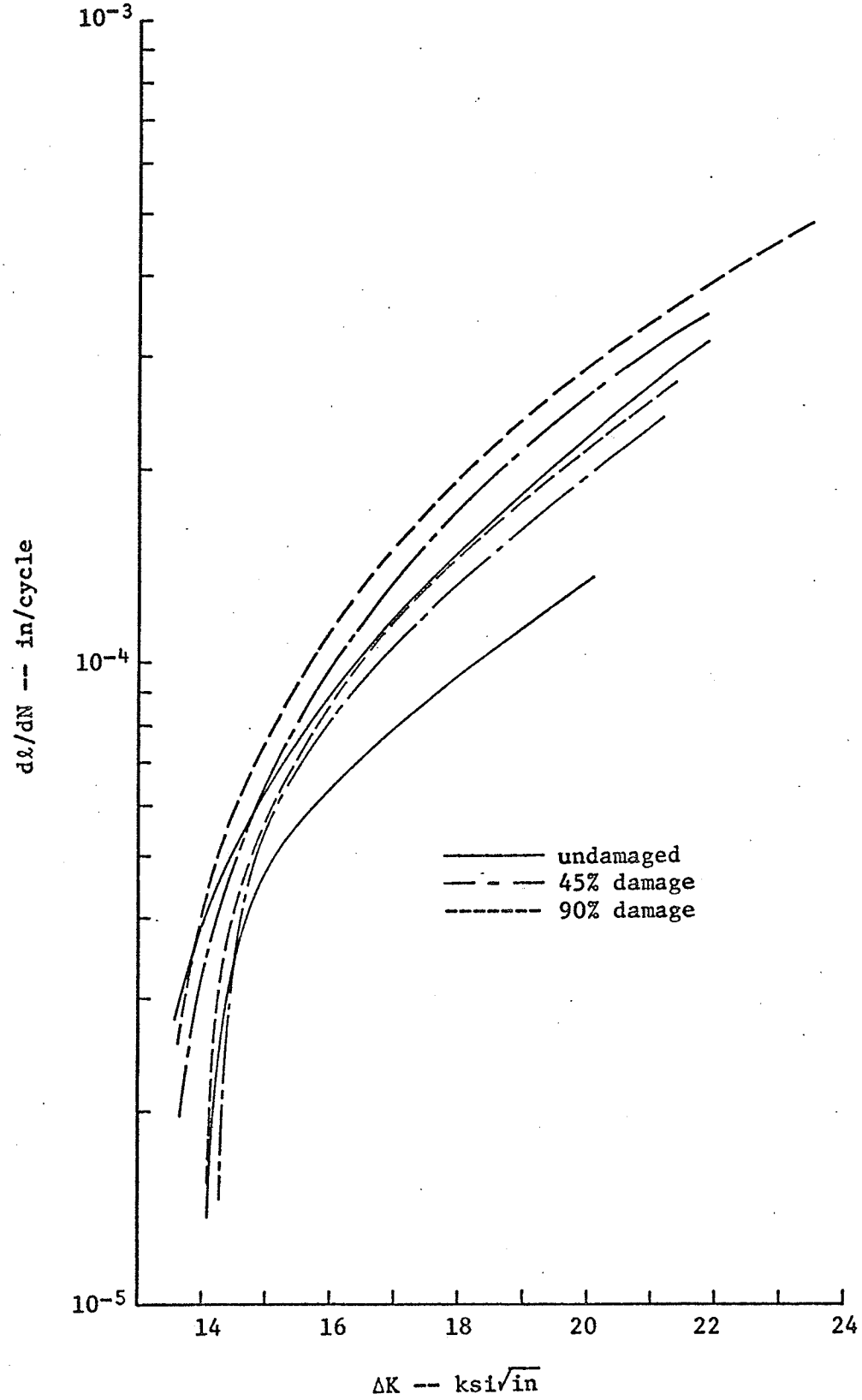

FIGURE 26

2024-T3 dℓ/dN vs ΔK SCATTER

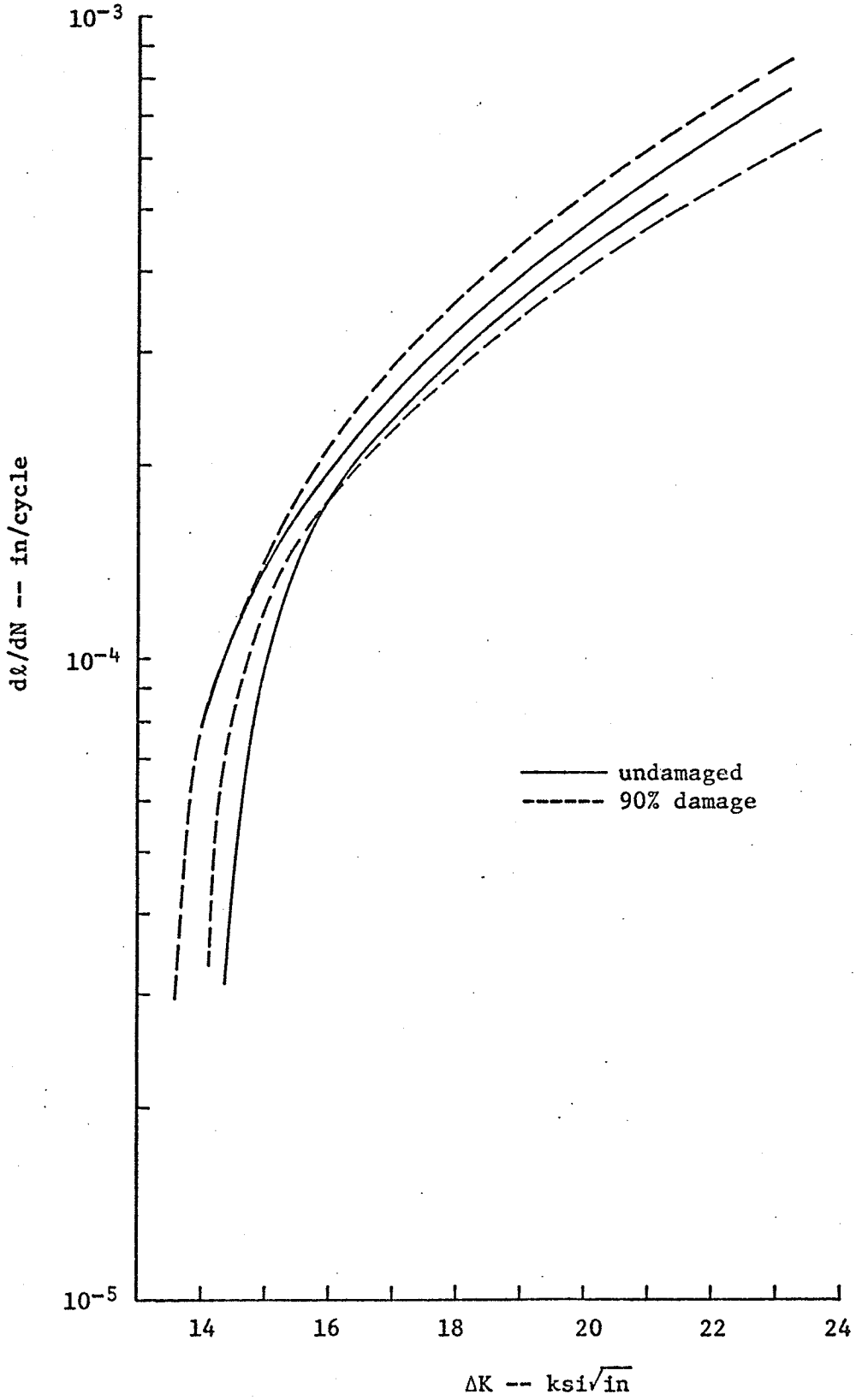

FIGURE 27

7075-T6 dℓ/dN vs ΔK SCATTER

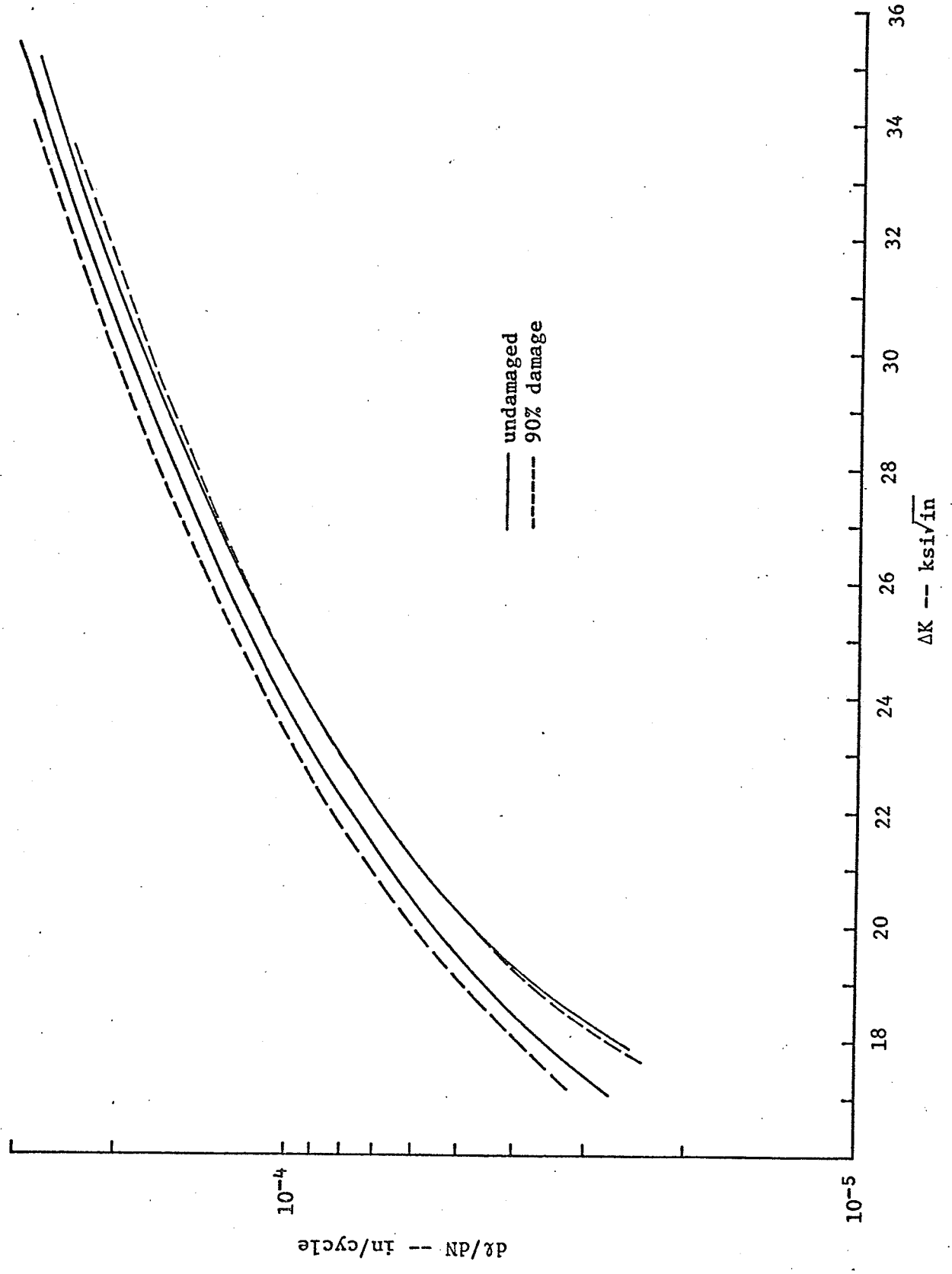

FIGURE 28

Ti-6Al-4V dℓ/dN vs ΔK SCATTER

APPENDIX A

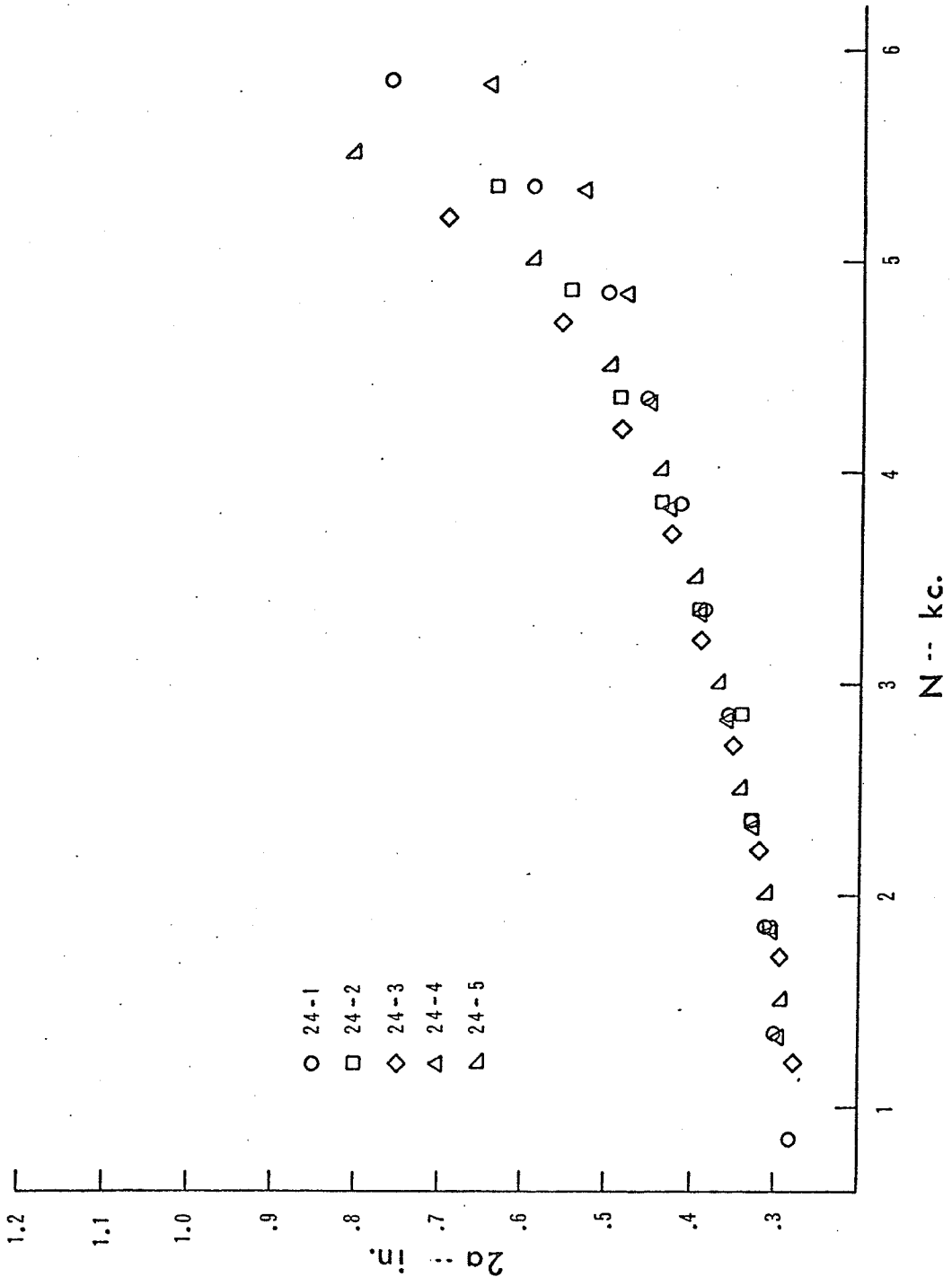

FIGURE AF-1

CRACK GROWTH - 2024-T3 UNDAMAGED

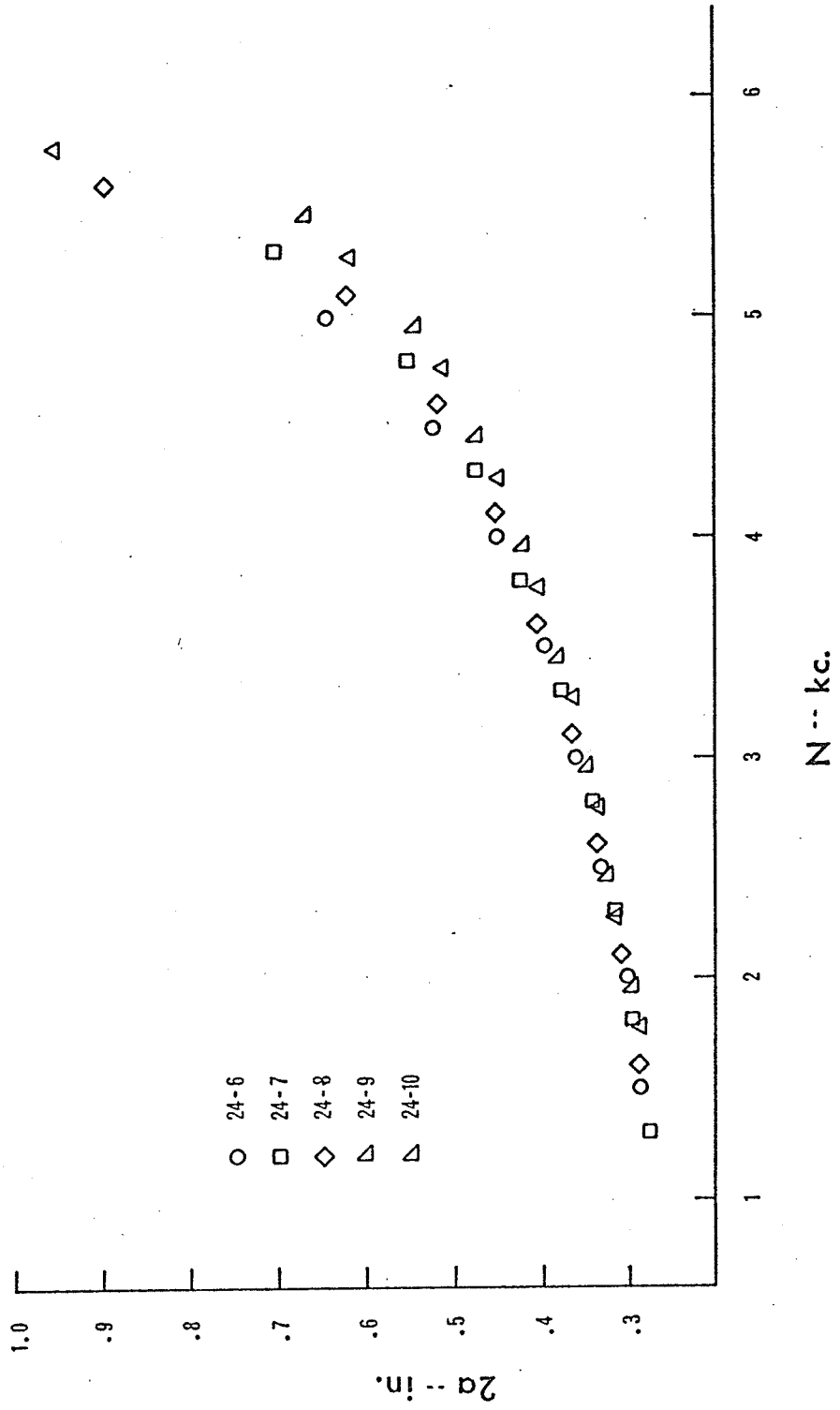

FIGURE AF-2

CRACK GROWTH - 2024-T3 45% DAMAGE

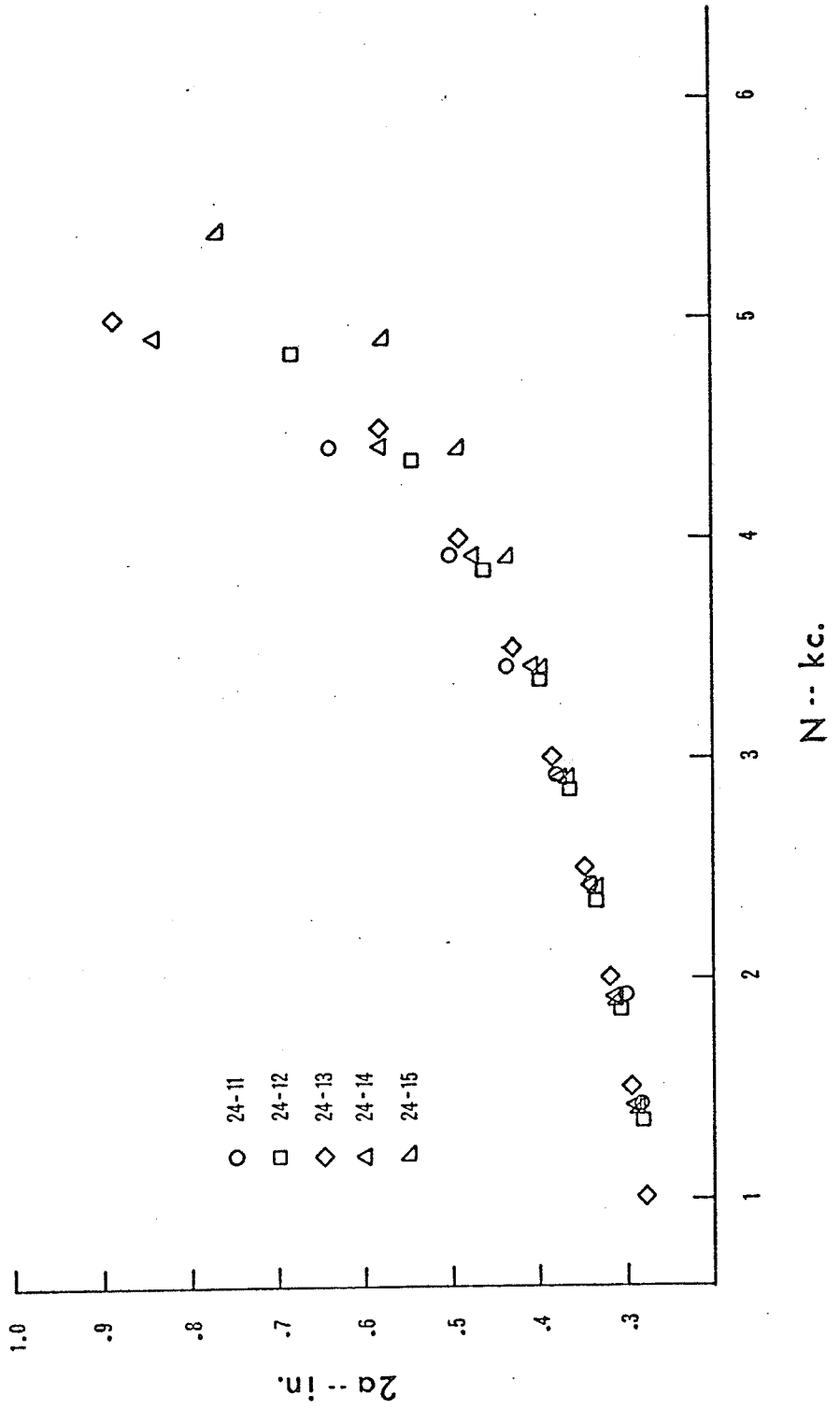

FIGURE AF-3

CRACK GROWTH - 2024-T3 90% DAMAGE

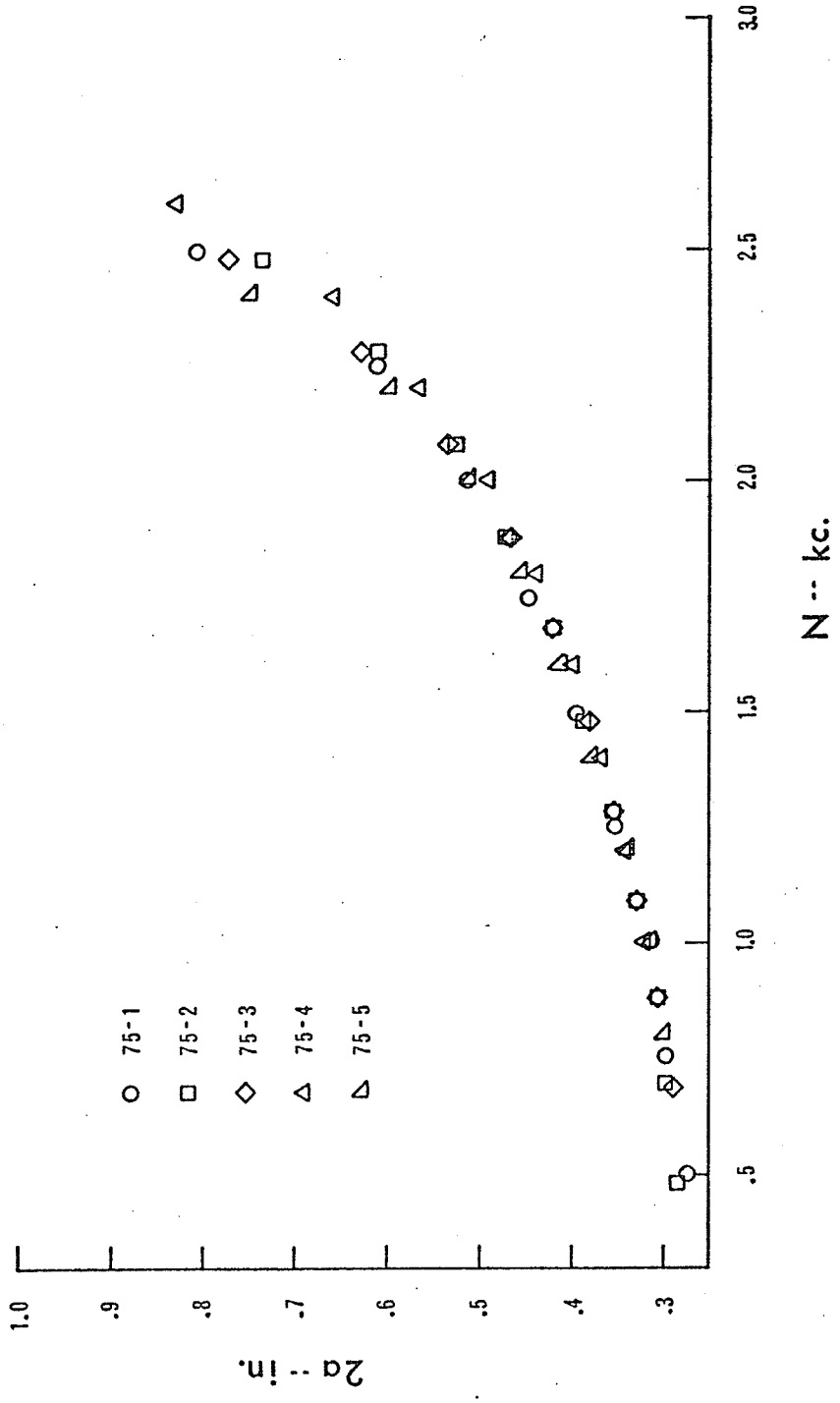

FIGURE AF-4

CRACK GROWTH - 7075-T6 UNDAMAGED

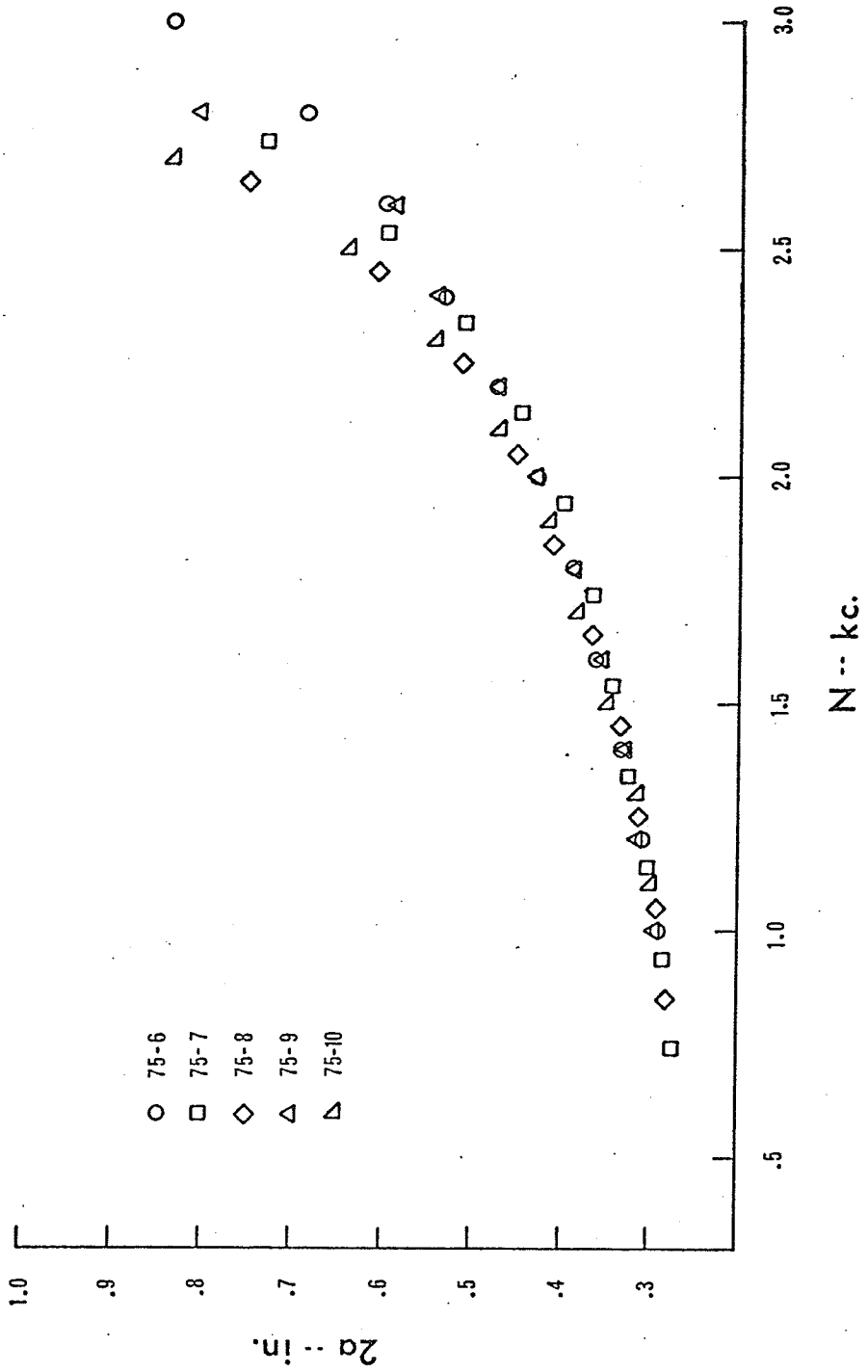

FIGURE AF-5

CRACK GROWTH - 7075-T6 90% DAMAGE

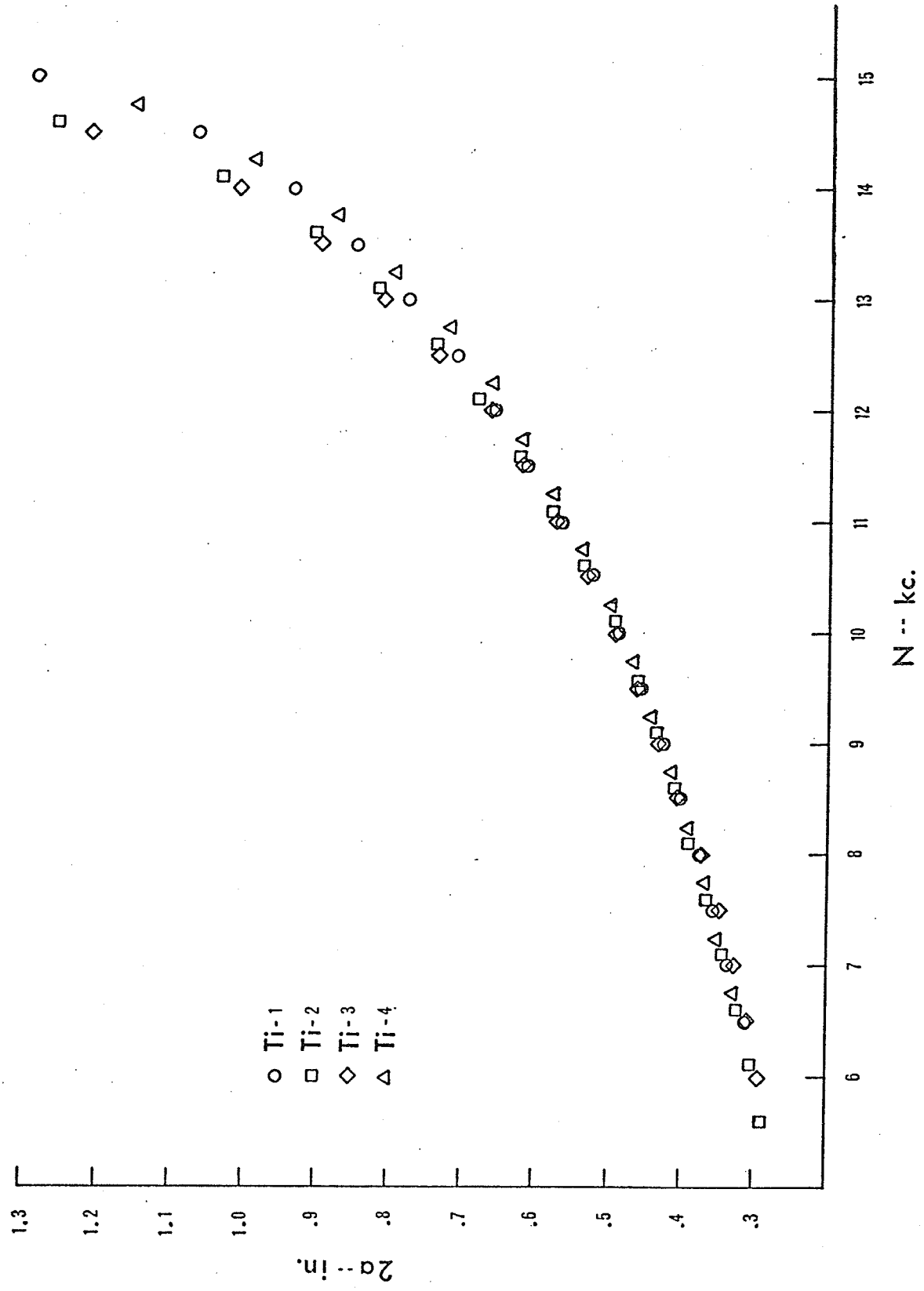

FIGURE AF-6

CRACK GROWTH - Ti-6Al-4V UNDAMAGED

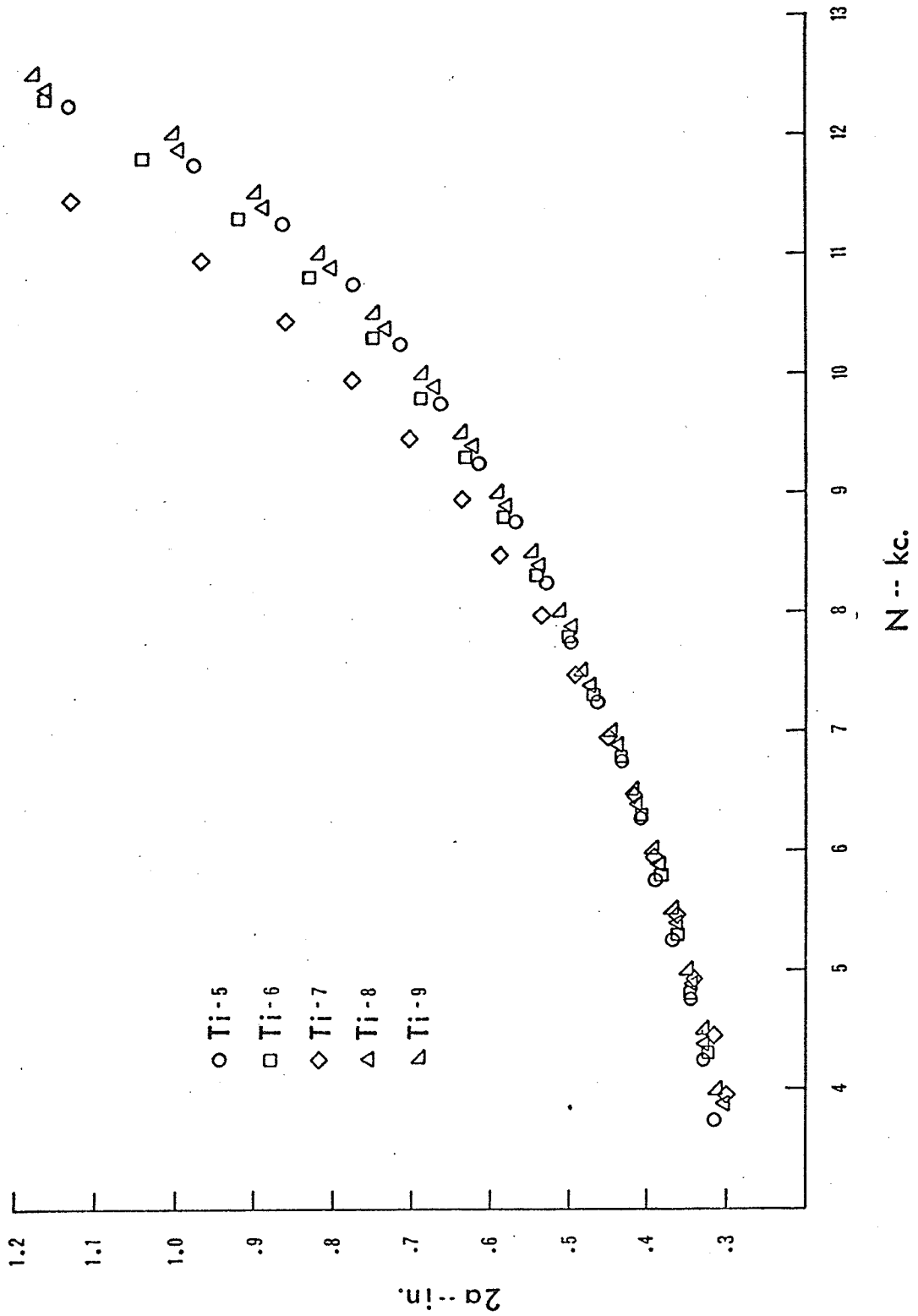

FIGURE AF-7

CRACK GROWTH - Ti-6Al-4V 90% DAMAGE

TABLE AT-1 CRACK MEASUREMENTS 2024-*T*3

PREFATIGUE
DAMAGE: 0 *PERCENT*
CYCLES: 0
STRESS: 13400±11840*PSI*

CRACK PROPOGATION
SECTION STRESS: 14578±12889*PSI*

TEST N CYCLES	24-1 *A CM.*	24-1 *N CYCLES*	24-2 *A CM.*	24-2 *N CYCLES*	24-3 *A CM.*	24-3 *N CYCLES*	24-4 *A CM.*	24-4 *N CYCLES*	24-5 *A CM.*	24-5 *N CYCLES*
0	0.631	0	0.683	0	0.641	0	0.650	0	0.644	
1500	0.720	850	0.788	1850	0.705	1200	0.743	1325	0.737	*R*
2000	0.765	1350	0.840	2350	0.747	1700	0.775	1825	0.789	*E*
2500	0.797	1850	0.918	2850	0.817	2200	0.837	2325	0.861	*F*
3000	0.840	2350	1.000	3350	0.893	2700	0.911	2825	0.932	*E*
3500	0.911	2850	1.111	3850	0.997	3200	1.000	3325	1.010	*R*
4000	0.983	3350	1.237	4350	1.088	3700	1.092	3825	1.112	*E*
4500	1.056	3850	1.390	4850	1.236	4200	1.151	4325	1.264	*N*
5000	1.155	4350	1.624	5350	1.420	4700	1.225	4825	1.501	*C*
5500	1.275	4850	-----	----	1.765	5200	1.355	5325	2.060	*E*
6000	1.508	5350	-----	----	-----	----	1.644	5825	-----	
6500	1.943	5850	-----	----	-----	----	-----	----	-----	

NOTE - ALL CRACK MEASUREMENTS WERE MADE AT THE INTERVALS SHOWN UNDER THE COLUMN N. DUE TO DELAYS IN THE INITIATION OF THE CRACK, IT WAS NECESSARY TO ADJUST FOR THIS IN COMPARING THE CRACK GROWTH. THE VALUES LISTED UNDER N REPRESENT THE ADJUSTED VALUE OF N.

TABLE AT-2 CRACK MEASUREMENTS 2024-T3

PREFATIGUE
DAMAGE: 45 *PERCENT*
CYCLES: 375000
STRESS: 13400±11840*PSI*

CRACK PROPOGATION
SECTION STRESS: 14578±12889*PSI*

TEST	24-6		24-7		24-8		24-9		24-10	
N CYCLES	*A CM.*	*N CYCLES*	*A CM.*	*N CYCLES*	*A CM.*	*N CYCLES*	*A CM.*	*N CYCLES*	*A CM.*	*N CYCLES*
0	0.622		0.632	0	0.630	0	0.664	0	0.646	0
1000	-----	*R*	0.705	1300	-----	----	0.733	1775	-----	----
1500	0.730	*E*	0.755	1800	0.732	1600	0.803	2275	0.754	1950
2000	0.770	*F*	0.807	2300	0.786	2100	0.857	2775	0.828	2450
2500	0.839	*E*	0.865	2800	0.858	2600	0.930	3275	0.888	2950
3000	0.920	*R*	0.965	3300	0.929	3100	1.028	3775	0.975	3450
3500	1.009	*E*	1.081	3800	1.033	3600	1.146	4275	1.075	3950
4000	1.149	*N*	1.215	4300	1.145	4100	1.305	4775	1.209	4450
4500	1.328	*C*	1.409	4800	1.318	4600	1.573	5275	1.384	4950
5000	1.638	*E*	1.792	5300	1.576	5100	2.426	5775	1.697	5450
5500	-----		-----	----	2.282	5600	-----	----	-----	----

TABLE AT-3 CRACK MEASUREMENTS 2024-T3

PREFATIGUE
DAMAGE: 90 PERCENT
CYCLES: 750000
STRESS: 13400±11840PSI

CRACK PROPOGATION
SECTION STRESS: 14578±12889PSI

TEST N CYCLES	24-11 A CM.	24-11 N CYCLES	24-12 A CM.	24-12 N CYCLES	24-13 A CM.	24-13 N CYCLES	24-14 A CM.	24-14 N CYCLES	24-15 A CM.	24-15 N CYCLES
0	0.645	0	0.648	0	0.632		0.654	0	0.641	0
1000	0.725	1425	0.710	1350	0.705	R	0.737	1425	0.725	1400
1500	0.769	1925	0.783	1850	0.748	E	0.787	1925	0.794	1900
2000	0.865	2425	0.844	2350	0.805	F	0.866	2425	0.860	2400
2500	0.965	2925	0.925	2850	0.879	E	0.945	2925	0.931	2900
3000	1.110	3425	1.012	3350	0.980	R	1.040	3425	1.014	3400
3500	1.272	3925	1.175	3850	1.093	E	1.205	3925	1.107	3900
4000	1.625	4425	1.385	4350	1.249	N	1.472	4425	1.249	4400
4500	-----	----	1.735	4850	1.479	C	2.141	4925	1.469	4900
5000	-----	----	-----	----	2.246	E	-----	----	1.947	5400

TABLE AT-4 CRACK MEASUREMENTS 7075-T6

PREFATIGUE
DAMAGE: 0 *PERCENT*
CYCLES: 0
STRESS: 13400±11840*PSI*

CRACK PROPOGATION
SECTION STRESS: 14578±12889*PSI*

TEST	75-1		75-2		75-3		75-4		75-5	
N CYCLES	*A CM.*	*N CYCLES*	*A CM.*	*N CYCLES*	*A CM.*	*N CYCLES*	*A CM.*	*N CYCLES*	*A CM.*	*N CYCLES*
0	0.630	0	0.650	0	0.660	0	0.690		0.660	----
800	0.699	500	0.727	480	0.738	680	0.785	*R*	0.764	----
1000	0.757	750	0.759	680	0.781	880	0.830	*E*	0.825	----
1200	0.802	1000	0.788	880	0.845	1080	0.870	*F*	0.876	----
1400	0.903	1250	0.841	1080	0.904	1280	0.938	*E*	0.969	----
1600	1.006	1500	0.912	1280	0.982	1480	1.012	*R*	1.058	----
1800	1.137	1750	0.991	1480	1.068	1680	1.120	*E*	1.163	----
2000	1.310	2000	1.076	1680	1.191	1880	1.247	*N*	1.305	----
2200	1.551	2250	1.188	1880	1.363	2080	1.436	*C*	1.518	----
2400	2.051	2500	1.342	2080	1.595	2280	1.671	*E*	1.906	----
2600	-----	----	1.549	2280	1.960	2480	2.110		-----	----
2800	-----	----	1.870	2480	-----	----	-----		-----	----

TABLE AT-5 CRACK MEASUREMENTS 7075-T6

PREFATIGUE
DAMAGE: 90 *PERCENT*
CYCLES: 400000
STRESS: 13400±11840*PSI*

CRACK PROPOGATION
SECTION STRESS: 14578±12889*PSI*

TEST	75-6		75-7		75-8		75-9		75-10	
N CYCLES	*A CM.*	*N CYCLES*	*A CM.*	*N CYCLES*	*A CM.*	*N CYCLES*	*A CM.*	*N CYCLES*	*A CM.*	*N CYCLES*
0	0.626		0.640	0	0.654	0	0.693	0	0.655	0
600	0.000		0.690	740	-----	----	0.746	1000	-----	----
800	0.000	*R*	0.720	940	0.711	850	0.797	1200	0.750	1100
1000	0.730	*E*	0.766	1140	0.746	1050	0.837	1400	0.790	1300
1200	0.780	*F*	0.821	1340	0.796	1250	0.894	1600	0.879	1500
1400	0.842	*E*	0.866	1540	0.846	1450	0.980	1800	0.970	1700
1600	0.915	*R*	0.928	1740	0.928	1650	1.086	2000	1.055	1900
1800	0.982	*E*	1.013	1940	1.038	1850	1.202	2200	1.193	2100
2000	1.090	*N*	1.132	2140	1.147	2050	1.364	2400	1.375	2300
2200	1.200	*C*	1.296	2340	1.298	2250	1.612	2600	1.620	2500
2400	1.358	*E*	1.520	2540	1.542	2450	2.049	2800	2.122	2700
2600	1.517		1.855	2740	1.906	2650	-----	----	-----	----
2800	1.746		-----	----	-----	----	-----	----	-----	----
3000	2.118		-----	----	-----	----	-----	----	-----	----

TABLE AT-6 CRACK MEASUREMENTS TI-6AL-4V

PREFATIGUE
DAMAGE: 0 PERCENT
CYCLES: 0
STRESS: 29400±26880PSI

CRACK PROPOGATION
SECTION STRESS: 17778±16644PSI

TEST N CYCLES	TI-1 A CM.	TI-1 N CYCLES	TI-2 A CM.	TI-2 N CYCLES	TI-3 A CM.	TI-3 N CYCLES	TI-4 A CM.	TI-4 N CYCLES
0	0.640		0.612	0	0.645	0	6.300	0
3000	-----		0.730	6600	-----	----	-----	----
3500	-----		0.767	7100	-----	----	-----	----
4000	-----		0.818	7600	0.744	7000	-----	----
4500	-----		0.864	8100	0.784	7500	-----	----
5000	-----		0.918	8600	0.828	8000	-----	----
5500	-----		0.959	9100	0.879	8500	0.833	7750
6000	-----		1.039	9600	0.956	9000	0.888	8250
6500	-----		1.101	10100	1.022	9500	0.933	8750
7000	-----	R	1.168	10600	1.088	10000	0.991	9250
7500	0.791	E	1.268	11100	1.164	10500	1.055	9750
8000	0.850	F	1.366	11600	1.249	11000	1.123	10250
8500	0.900	E	1.468	12100	1.338	11500	1.185	10750
9000	0.950	R	1.585	12600	1.447	12000	1.265	11250
9500	1.011	E	1.730	13100	1.561	12500	1.364	11750
10000	1.082	N	1.877	13600	1.708	13000	1.462	12250
10500	1.157	C	2.062	14100	1.868	13500	1.575	12750
11000	1.236	E	2.306	14600	2.060	14000	1.685	13250
11500	1.330		2.630	15100	2.282	14500	1.827	13750
12000	1.435		3.202	15600	2.568	15000	2.022	14250
12500	1.556		-----	----	3.083	15500	2.221	14750
13000	1.672		-----	----	-----	----	2.510	15250
13500	1.804		-----	----	-----	----	2.922	15750
14000	1.968		-----	----	-----	----	-----	----
14500	2.157		-----	----	-----	----	-----	----
15000	2.372		-----	----	-----	----	-----	----
15500	2.713		-----	----	-----	----	-----	----
16000	3.273		-----	----	-----	----	-----	----

TABLE AT-7 CRACK MEASUREMENTS TI-6AL-4V

PREFATIGUE
DAMAGE: 90 PERCENT
CYCLES: 400000
STRESS: 29400±26880PSI

CRACK PROPOGATION
SECTION STRESS: 17778±16644PSI

TEST N CYCLES	TI-5 A CM.	TI-5 N CYCLES	TI-6 A CM.	TI-6 N CYCLES	TI-7 A CM.	TI-7 N CYCLES	TI-8 A CM.	TI-8 N CYCLES	TI-9 A CM.	TI-9 N CYCLES
0	0.631	0	0.609	0	0.628	0	0.650	0	0.628	
3000	-----	----	-----	----	-----	----	0.774	3875	-----	
3500	-----	----	-----	----	0.762	4950	0.820	4375	-----	
4000	0.798	3750	-----	----	0.807	5450	0.870	4875	0.788	
4500	0.828	4250	-----	----	0.867	5950	0.924	5375	0.834	
5000	0.875	4750	-----	----	0.928	6450	0.976	5875	0.880	
5500	0.936	5250	-----	----	0.989	6950	1.046	6375	0.938	
6000	0.989	5750	-----	----	1.058	7450	1.114	6875	1.000	R
6500	1.037	6250	-----	----	1.147	7950	1.196	7375	1.061	E
7000	1.100	6750	-----	----	1.252	8450	1.268	7875	1.132	F
7500	1.175	7250	-----	----	1.358	8950	1.361	8375	1.223	E
8000	1.260	7750	0.818	4300	1.480	9450	1.466	8875	1.296	R
8500	1.338	8250	0.877	4800	1.612	9950	1.570	9375	1.387	E
9000	1.438	8750	0.920	5300	1.785	10450	1.700	9875	1.495	N
9500	1.553	9250	0.975	5800	1.966	10950	1.858	10375	1.613	C
10000	1.682	9750	1.036	6300	2.186	11450	2.036	10875	1.745	E
10500	1.815	10250	1.106	6800	2.458	11950	2.242	11375	1.895	
11000	1.969	10750	1.190	7300	2.870	12450	2.526	11875	2.077	
11500	2.193	11250	1.273	7800	-----	----	2.948	12375	2.248	
12000	2.477	11750	1.366	8300	-----	----	-----	----	2.558	
12500	2.880	12250	1.480	8800	-----	----	-----	----	2.984	
13000	-----	----	1.604	9300	-----	----	-----	----	-----	
13500	-----	----	1.744	9800	-----	----	-----	----	-----	
14000	-----	----	1.902	10300	-----	----	-----	----	-----	
14500	-----	----	2.100	10800	-----	----	-----	----	-----	
15000	-----	----	2.338	11300	-----	----	-----	----	-----	
15500	-----	----	2.646	11800	-----	----	-----	----	-----	
16000	-----	----	3.080	12300	-----	----	-----	----	-----	

APPENDIX B

REDUCTION OF DATA

The crack propagation rate was evaluated by performing a polynomial regression analysis on the ℓ vs. N data to obtain an expression of the form:

$$\ell = F(N) \quad \text{---------- (B-1)}$$

and then differentiating

$$d\ell/dN = d\{F(N)\}/dN \quad \text{---------- (B-2)}$$

It was found that the best fit was obtained using an expression of the form:

$$\ell = \exp\{f(n)\} \quad \text{---------- (B-3)}$$

where n is kilocycles.

A standard library routine was modified to perform the regression analysis. This was done by performing a polynomial regression on the natural logarithm of the crack length ($\ln \ell$) and the number of cycles expressed in kilocycles (n).

$$\text{i.e. } \ln\ell = f(n) \quad \text{---------- (B-4)}$$

It was found that, in all instances, a second order polynomial gave the best fit to the data and the crack length was given by:

$$\ell = \exp(\alpha + \beta n + \gamma n^2) \quad \text{---------- (B-5)}$$

The crack propagation rate was therefore given by:

$$d\ell/dN = .001 d\ell/dn = .001(\beta+2\gamma n)\exp(\alpha+\beta n+\gamma n^2) \quad \text{------- (B-6)}$$

The regression was performed on each individual test and on the lumped data for each series of five tests.

From the regression equations, the crack length and the crack propogation rate were evaluated at specific intervals of N. To simplify the calculations, the alternating stress intensity factor was evaluated at each point using equation 5 (i.e. the finite width correction factor

was neglected in the calculations) but using the total crack length ℓ instead of the half length a. The constant π was further omitted in the calculations. The net result of these approximations was a calculated stress intensity factor fairly close in numerical value to the exact value suggested by Isida; for the range of crack length/width considered, the approximate value is slightly lower than the exact as shown in Appendix C, Tables CT-1 through CT-7.

The resulting ΔK vs. $d\ell/dN$ values are plotted in Appendix C as Figures CF-1 through CF-7. Also included in Appendix C are the numerical values used in obtaining the above curves.

APPENDIX C

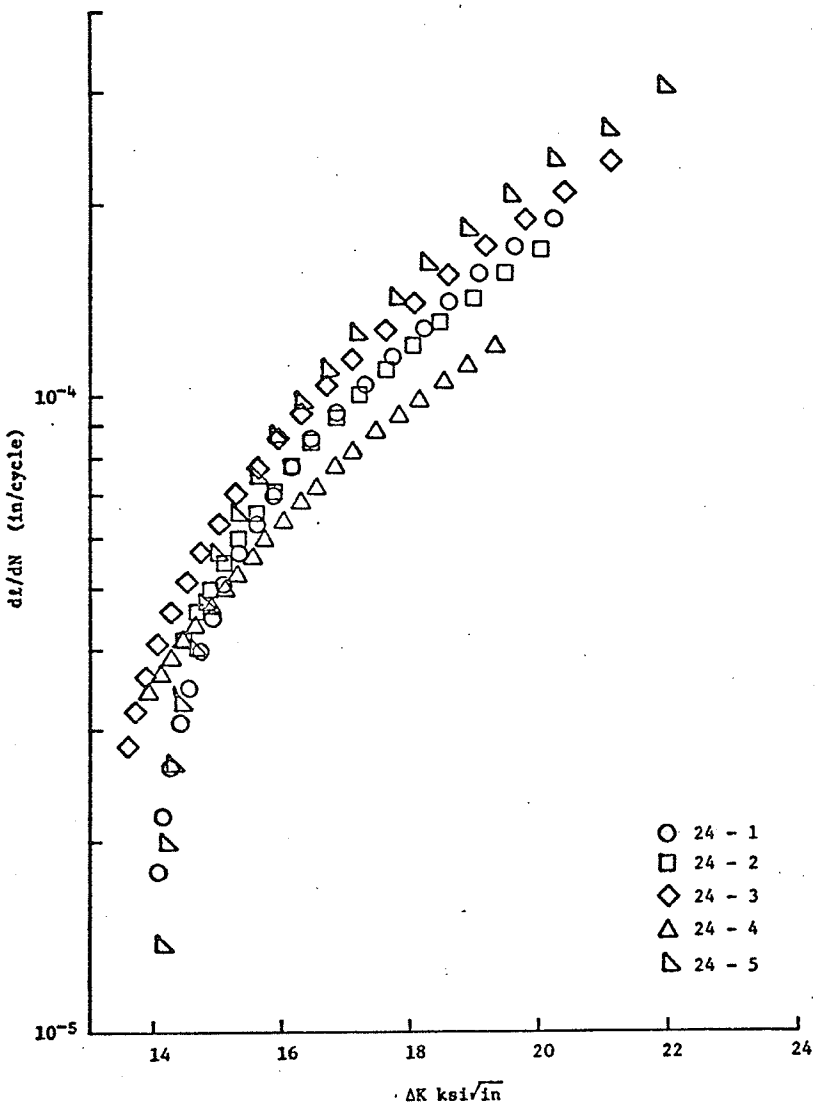

FIGURE CF-1

REDUCED RESULTS - 2024-T3 UNDAMAGED

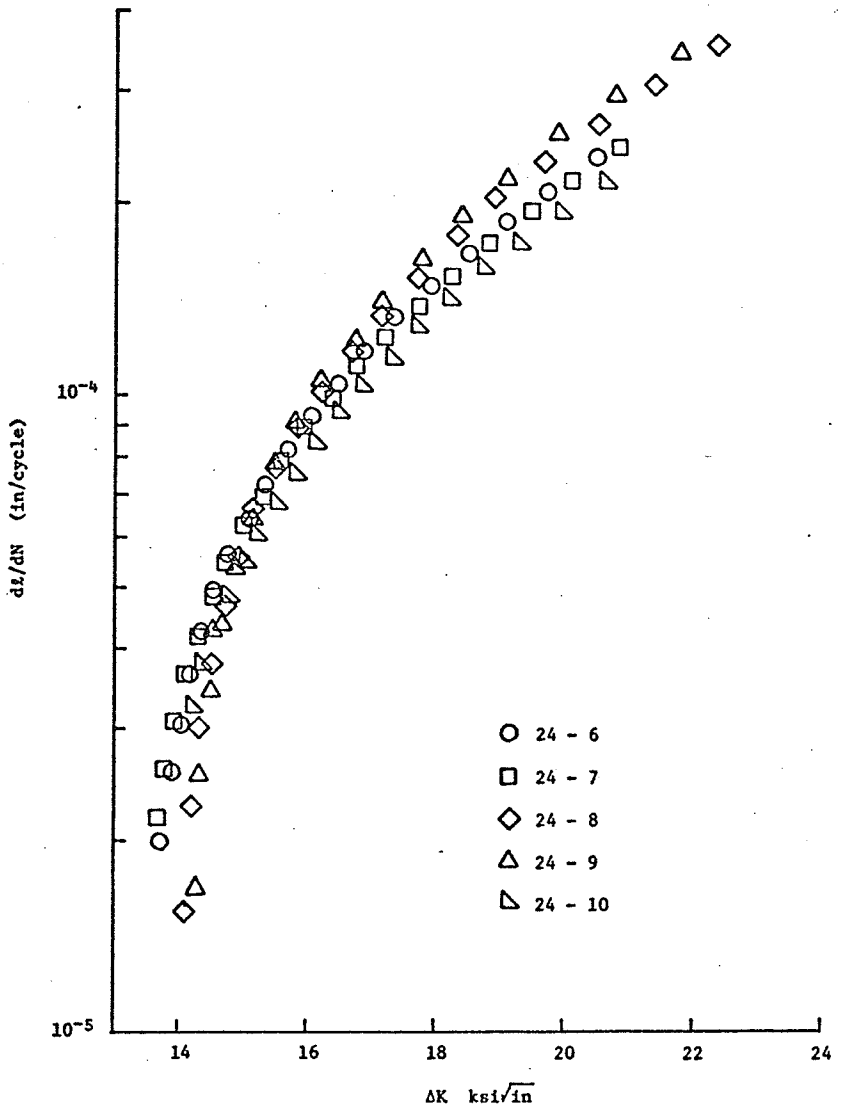

FIGURE CF-2

REDUCED RESULTS - 2024-T3 45% DAMAGE

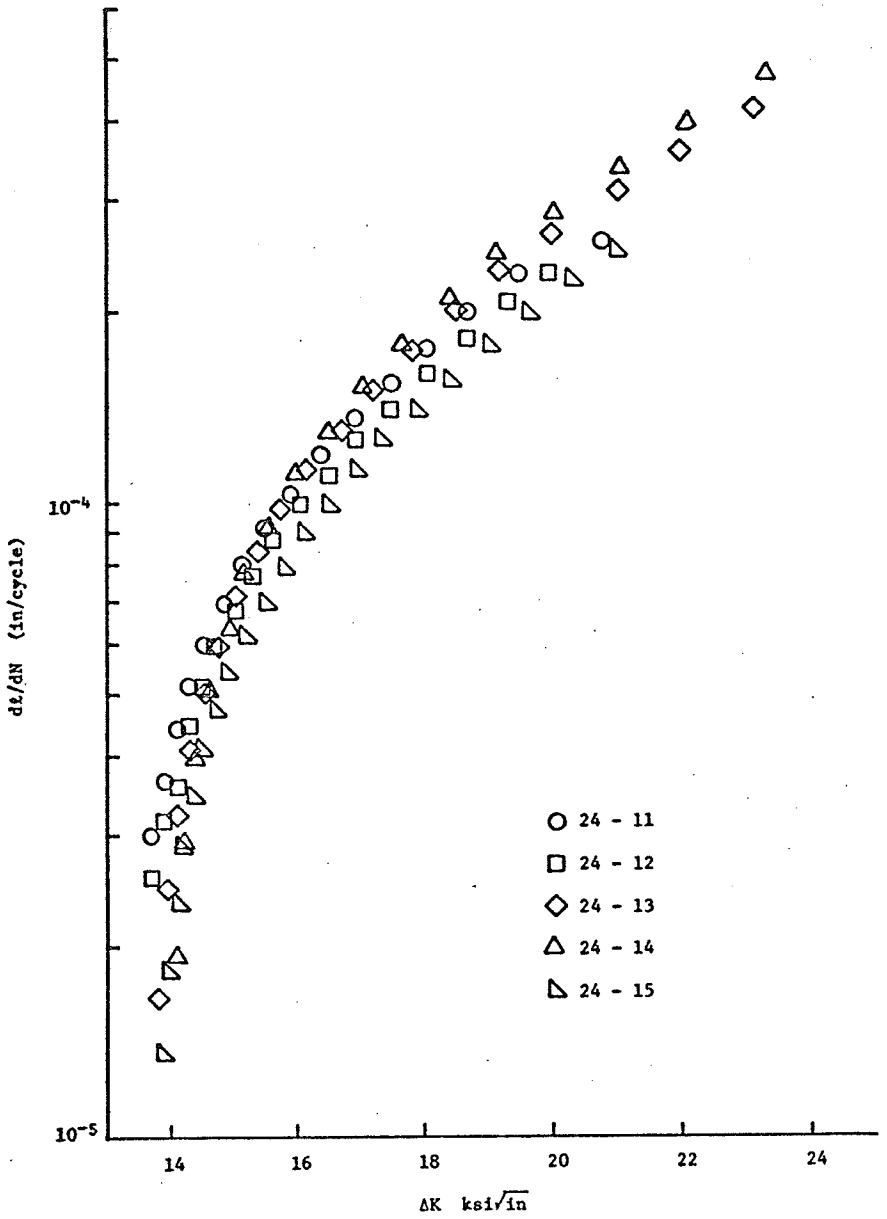

FIGURE CF-3

REDUCED RESULTS - 2024-T3 90% DAMAGE

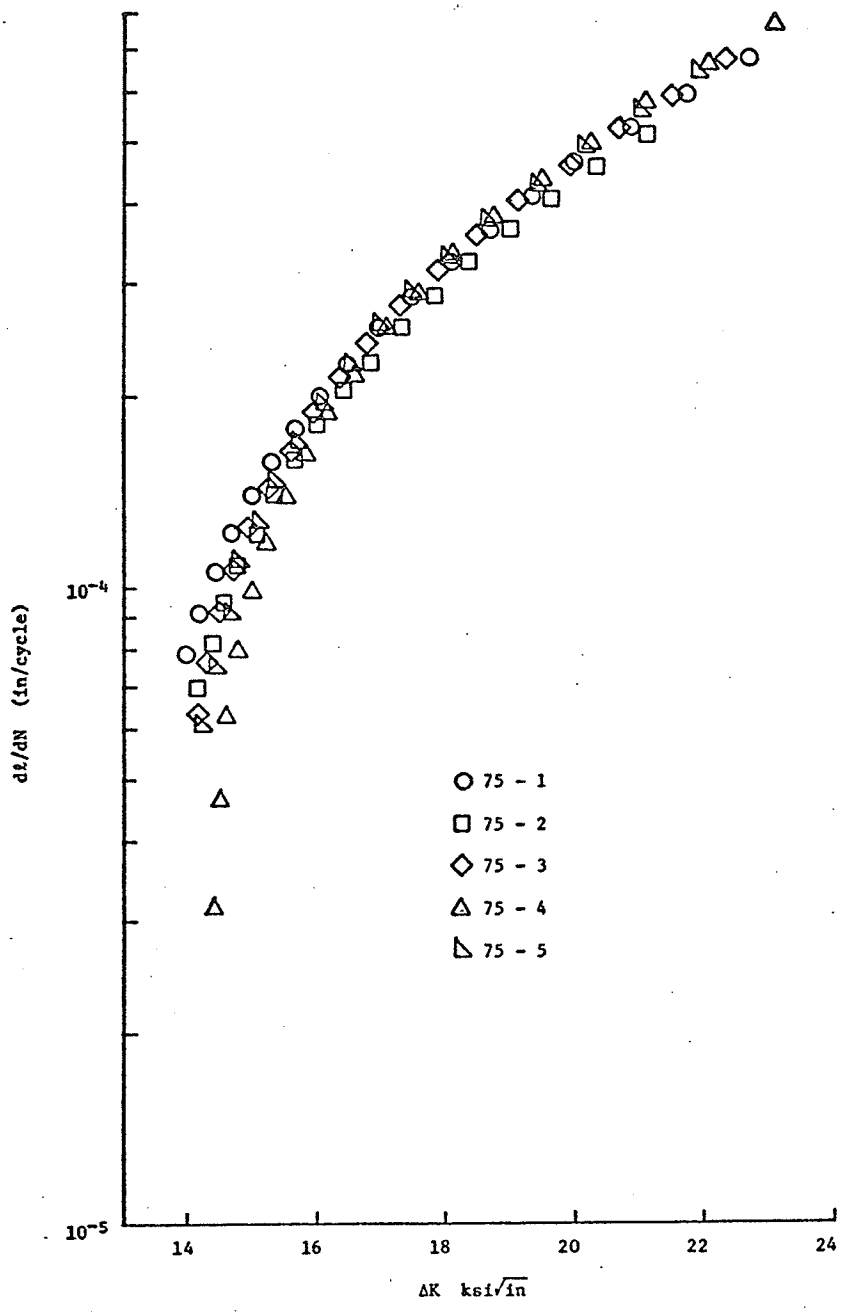

FIGURE CF-4

REDUCED RESULTS - 7075-T6 UNDAMAGED

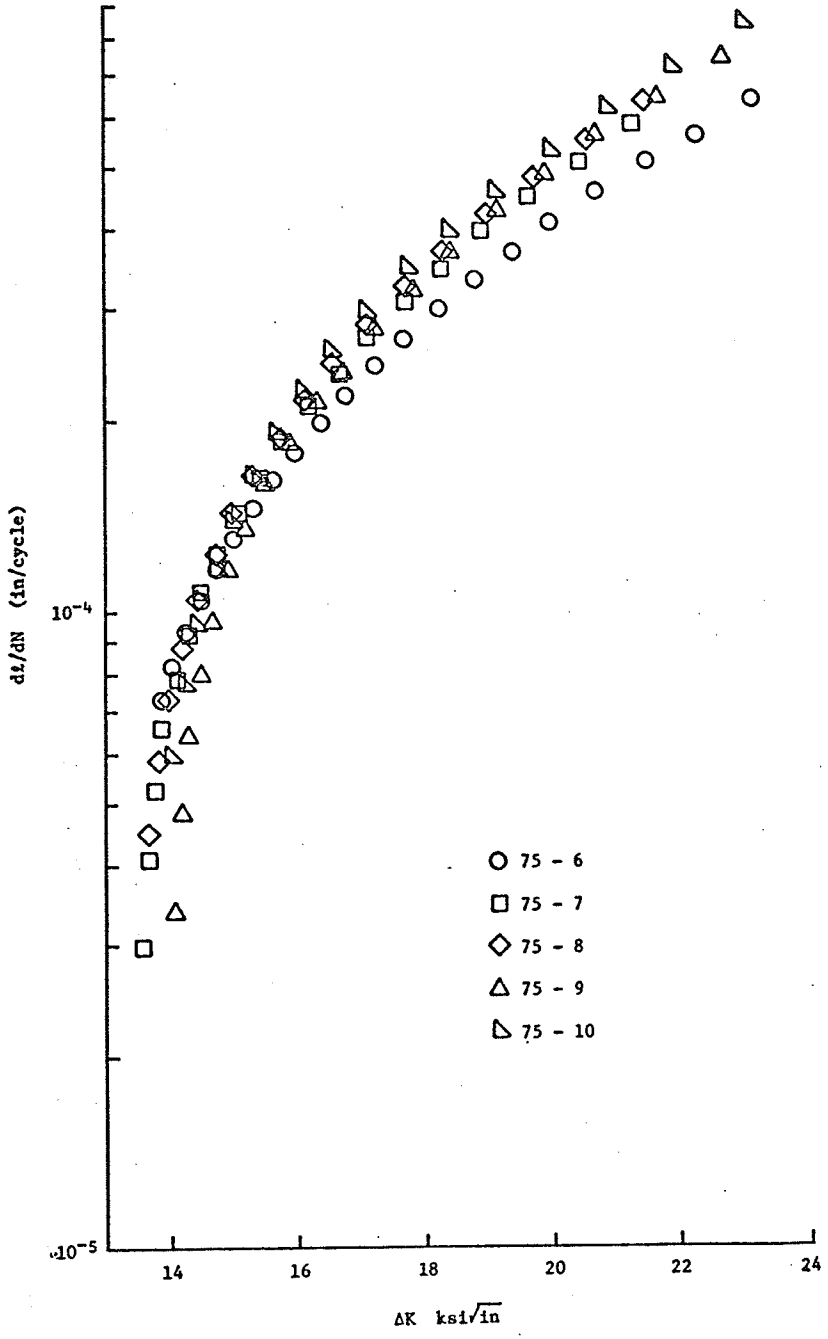

FIGURE CF-5

REDUCED RESULTS - 7075-T6 90% DAMAGE

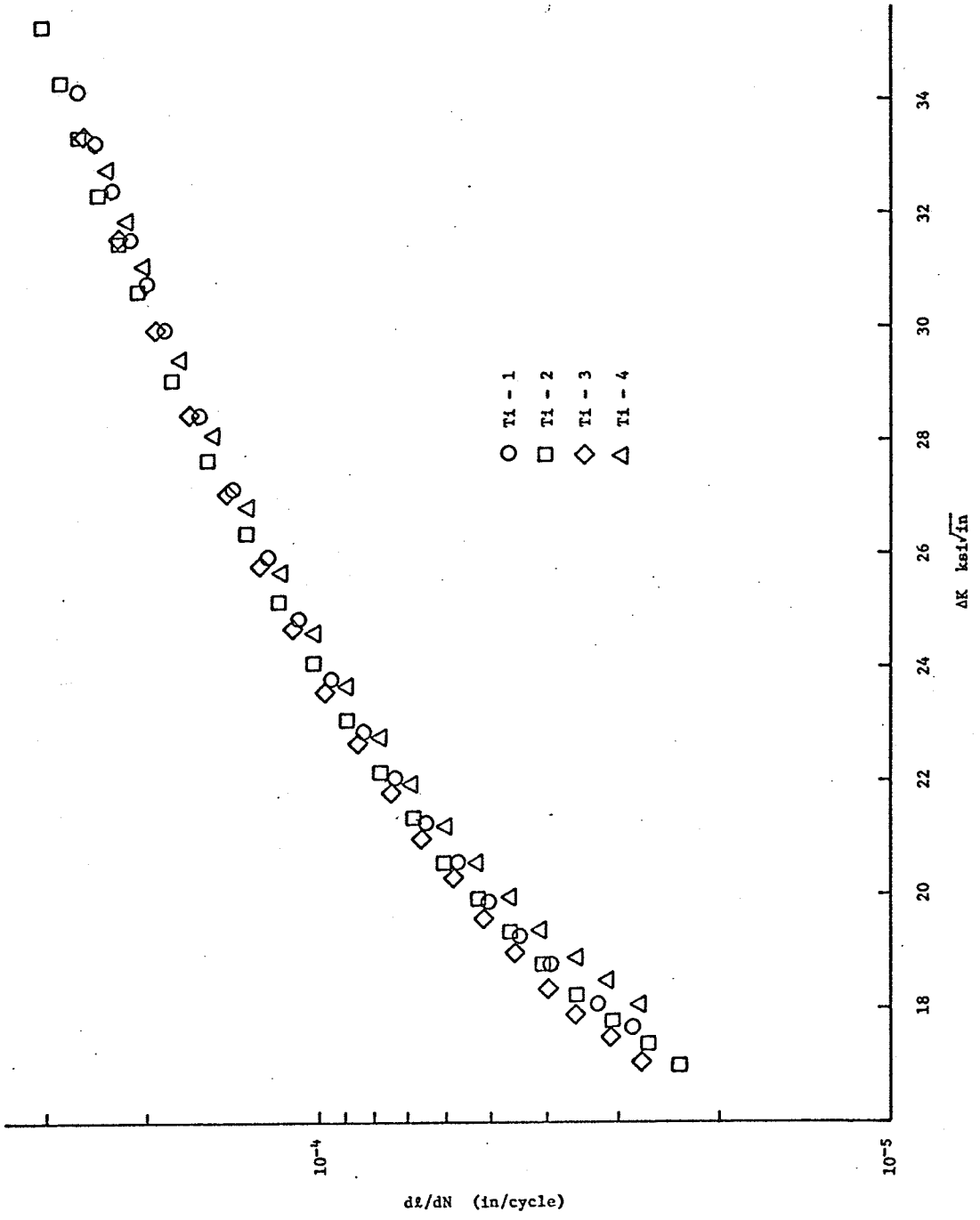

FIGURE CF-6

REDUCED RESULTS - Ti-6Al-4V UNDAMAGED

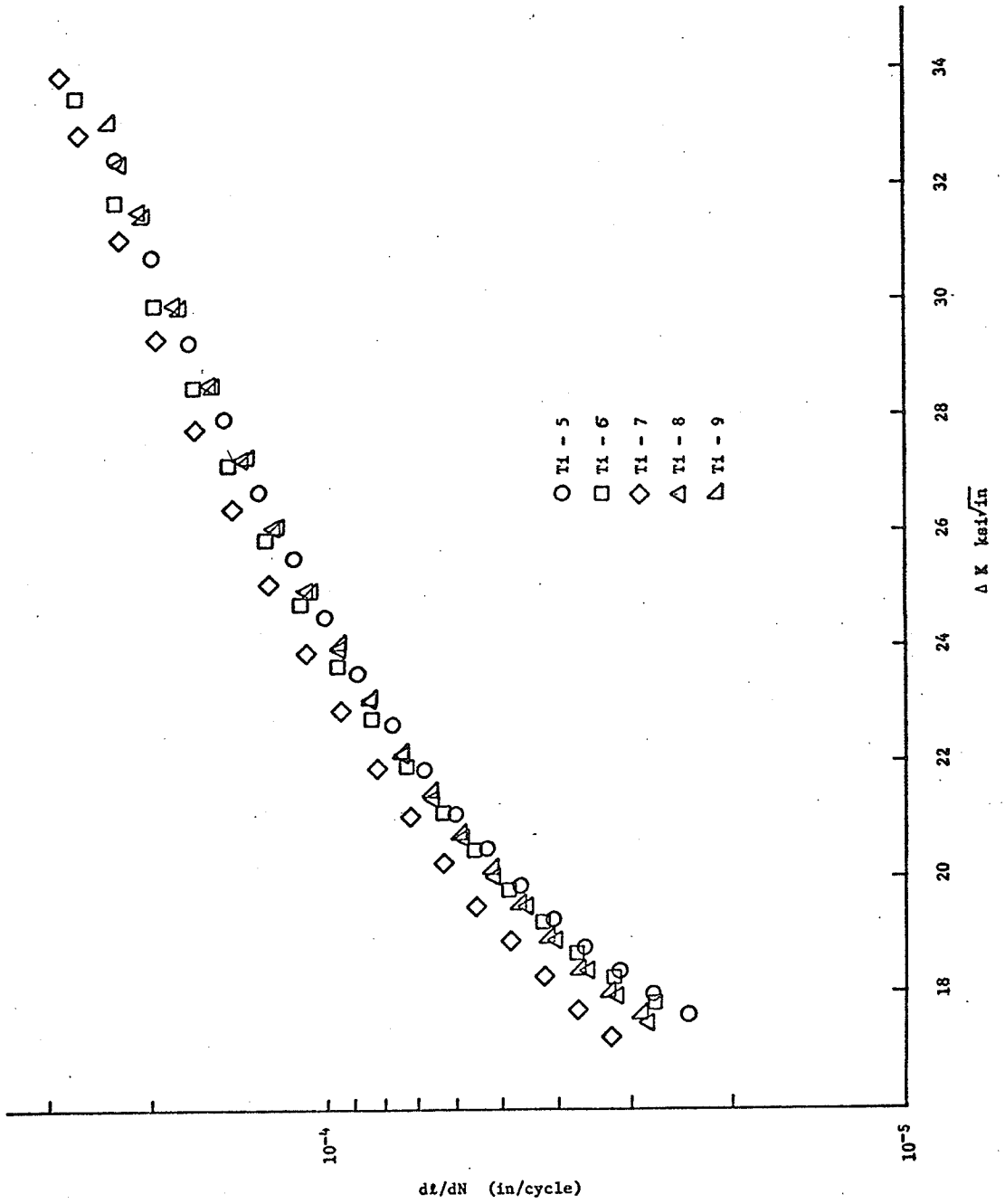

FIGURE CF-7

REDUCED RESULTS - Ti-6Al-4V 90% DAMAGE

TABLE CT-1

2024 *DA/DN VS* ΔK

UNDAMAGED			50*PC DAMAGE*			100*PC DAMAGE*		
DA/DN [1]	ΔK[2] (*APPROX*)	ΔK (*EXACT*)[3]	*DA/DN*	ΔK (*APPROX*)	ΔK (*EXACT*)	*DA/DN*	ΔK (*APPROX*)	ΔK (*EXACT*)
0.2269	1.3693	1.7242	0.1026	1.3887	1.7492	0.1669	1.3625	1.7156
0.2579	1.3809	1.7392	0.1592	1.3949	1.7572	0.2191	1.3719	1.7276
0.2904	1.3940	1.7560	0.2177	1.4038	1.7686	0.2735	1.3837	1.7428
0.3247	1.4085	1.7746	0.2786	1.4154	1.7835	0.3310	1.3981	1.7613
0.3611	1.4245	1.7952	0.3429	1.4299	1.8022	0.3921	1.4150	1.7830
0.3996	1.4421	1.8179	0.4112	1.4472	1.8245	0.4576	1.4348	1.8085
0.4407	1.4612	1.8426	0.4845	1.4675	1.8507	0.5283	1.4573	1.8376
0.4845	1.4820	1.8695	0.5638	1.4909	1.8810	0.6052	1.4828	1.8705
0.5316	1.5045	1.8986	0.6500	1.5176	1.9157	0.6892	1.5114	1.9076
0.5821	1.5288	1.9302	0.7447	1.5477	1.9548	0.7816	1.5432	1.9490
0.6366	1.5549	1.9642	0.8490	1.5813	1.9987	0.8836	1.5784	1.9949
0.6955	1.5830	2.0008	0.9647	1.6188	2.0478	0.9970	1.6173	2.0458
0.7592	1.6131	2.0403	1.0937	1.6603	2.1024	1.1234	1.6601	2.1021
0.8284	1.6453	2.0826	1.2382	1.7061	2.1630	1.2648	1.7070	2.1642
0.9036	1.6797	2.1281	1.4008	1.7564	2.2300	1.4238	1.7582	2.2324
0.9855	1.7165	2.1768	1.5843	1.8117	2.3042	1.6031	1.8142	2.3076
1.0750	1.7558	2.2291	1.7924	1.8723	2.3864	1.8059	1.8753	2.3905
1.1728	1.7976	2.2852	2.0291	1.9385	2.4772	2.0361	1.9418	2.4817
1.2799	1.8421	2.3454	2.2993	2.0110	2.5781	2.2982	2.0142	2.5825
1.3975	1.8896	2.4100	2.6088	2.0900	2.6899	2.5974	2.0930	2.6942
1.5268	1.9401	2.4794	2.9643	2.1763	2.8148	2.9400	2.1786	2.8182
1.6691	1.9938	2.5539				3.3334	2.2718	2.9569
1.8259	2.0509	2.6343				3.7863	2.3730	3.1127

[1] in/cycle$\times 10^{-4}$
[2] psi$\sqrt{\text{in}} \times 10^{5}$
[3] using Isida's finite width correction factor

TABLE CT-2

7075 *DA/DN VS ΔK*

UNDAMAGED			*100PC DAMAGE*		
DA/DN	*ΔK (APPROX)*	*ΔK (EXACT)*	*DA/DN*	*ΔK (APPROX)*	*ΔK (EXACT)*
0.6724	1.4166	1.7851	0.6837	1.3847	1.7440
0.8035	1.4337	1.8071	0.7998	1.4023	1.7667
0.9441	1.4537	1.8329	0.9246	1.4225	1.7927
1.0960	1.4767	1.8626	1.0593	1.4454	1.8222
1.2613	1.5028	1.8965	1.2058	1.4710	1.8553
1.4424	1.5323	1.9348	1.3660	1.4996	1.8923
1.6418	1.5652	1.9776	1.5421	1.5314	1.9336
1.8628	1.6018	2.0255	1.7364	1.5663	1.9791
2.1087	1.6422	2.0785	1.9519	1.6048	2.0294
2.3837	1.6868	2.1374	2.1918	1.6469	2.0847
2.6925	1.7358	2.2025	2.4598	1.6929	2.1455
3.0406	1.7895	2.2744	2.7603	1.7431	2.2122
3.4346	1.8484	2.3539	3.0983	1.7978	2.2855
3.8820	1.9126	2.4415	3.4797	1.8573	2.3660
4.3916	1.9828	2.5386	3.9114	1.9219	2.4543
4.9741	2.0594	2.6463	4.4013	1.9921	2.5516
5.6419	2.1428	2.7660	4.9590	2.0682	2.6588
6.4098	2.2338	2.8998	5.5953	2.1509	2.7777
			6.3234	2.2406	2.9100

TABLE CT-3

TI-6AL-4V DA/DN VS ΔK

UNDAMAGED			*100PC DAMAGE*		
DA/DN	*ΔK (APPROX)*	*ΔK (EXACT)*	*DA/DN*	*ΔK (APPROX)*	*ΔK (EXACT)*
0.2421	1.7065	2.1475	0.2460	1.7564	2.2114
0.2589	1.7243	2.1703	0.2650	1.7741	2.2342
0.2765	1.7432	2.1945	0.2849	1.7929	2.2583
0.2951	1.7631	2.2200	0.3060	1.8129	2.2840
0.3147	1.7841	2.2470	0.3282	1.8342	2.3114
0.3354	1.8062	2.2754	0.3517	1.8567	2.3404
0.3573	1.8295	2.3054	0.3765	1.8805	2.3711
0.3805	1.8540	2.3369	0.4028	1.9056	2.4036
0.4050	1.8797	2.3701	0.4307	1.9322	2.4380
0.4310	1.9066	2.4049	0.4604	1.9601	2.4742
0.4587	1.9349	2.4415	0.4920	1.9896	2.5126
0.4880	1.9646	2.4801	0.5257	2.0206	2.5530
0.5193	1.9947	2.5192	0.5615	2.0532	2.5956
0.5525	2.0282	2.5629	0.5999	2.0875	2.6406
0.5880	2.0623	2.6075	0.6408	2.1235	2.6879
0.6258	2.0979	2.6542	0.6847	2.1612	2.7376
0.6662	2.1352	2.7033	0.7316	2.2009	2.7902
0.7094	2.1742	2.7548	0.7819	2.2425	2.8455
0.7556	2.2150	2.8089	0.8360	2.2862	2.9039
0.8050	2.2576	2.8656	0.8940	2.3319	2.9653
0.8571	2.3021	2.9252	0.9564	2.3799	3.0302
0.9147	2.3487	2.9880	1.0236	2.4302	3.0986
0.9757	2.3974	3.0539	1.0959	2.4829	3.1708
1.0411	2.4482	3.1232	1.1739	2.5381	3.2471
1.1114	2.5013	3.1962	1.2581	2.5959	3.3278
1.1870	2.5568	3.2731	1.3490	2.6566	3.4134
1.2684	2.6148	3.3543	1.4472	2.7201	3.5040
1.3560	2.6754	3.4401	1.5535	2.7867	3.6003
1.4505	2.7387	3.5307	1.6687	2.8564	3.7027
1.5524	2.8049	3.6269	1.7934	2.9295	3.8120
1.6624	2.8741	3.7290	1.9287	3.0061	3.9289
1.7813	2.9463	3.8374	2.0755	3.0864	4.0543
1.9098	3.0219	3.9533	2.2350	3.1705	4.1891
2.0487	3.1008	4.0771	2.4084	3.2587	4.3349
2.1992	3.1834	4.2101	2.5972	3.3512	4.4933
2.3622	3.2697	4.3534			
2.5389	3.3600	4.5087			
2.7307	3.4545	4.6781			